AN EXPERIMENTAL STUDY OF VARIABLE VOLUME PNEUMATIC CAPACITORS

D. Vouloumanos

A MAJOR TECHNICAL REPORT

in the

Faculty of Engineering

Presented in partial fulfilment of the requirements for the Degree of Master of Engineering at
Concordia University
Montreal, Canada

March, 1975

AN EXPERIMENTAL STUDY OF VARIABLE VOLUME PNEUMATIC CAPACITORS

D. Vouloumanos

ABSTRACT

Fluid capacitors are widely used in the construction of oscillators and time delay circuits for industrial control systems. Their interaction with other active elements has not been studied extensively. This report presents an experimental study of the behaviour of the variable volume pneumatic capacitors when connected to a fluidic amplifier circuit. In comparing the theoretical curves with experimental results, it is shown that the experimental curves follow the theoretical ones fairly closely. During the charging process of the capacitor, the experimental curve follows first the adiabatic and then gradually tapers off towards the isothermal curve. During the discharging process, the theoretical curves calculated from different values of polytropic index are quite close to each other and exhibit a close correlation with the experimental curves. It is concluded that either adiabatic or isothermal polytropic indexes may be used to predict pressure drop during the discharging process without appreciable error.

ACKNOWLEDGEMENTS

I wish to acknowledge my debt to Dr. C.K. Kwok, my advisor, for his continuous help and guidance in completing my work.

I am also grateful to Mr. J. Elliott for his assistance in carrying out the experimental phase of my work in the Fluid Control Center.

TABLE OF CONTENTS

LIST OF TABLES

LIST OF FIGURES

CHAPTER 1

INTRODUCTION

The application of fluidic devices in the design of industrial pneumatic control systems has increased considerably in the last few years. Their simplicity, low cost and reliable performance have increased their popularity and acceptance in many applications. The practical application of fluidics in chemical processes in particular has been widely used because of their explosion proof quality. However, the continual increased use of fluidic systems has pointed out the necessity for a better understanding of the interaction mechanisms between fluid amplifier and passive elements such as resistors and capacitors.

Approximate values for the pneumatic capacitance of a fixed mass of air, isothermal and ideal isentropic compressions were derived by Ahrendt and Taplin [1] early in 1951. Helm [2] discussed some aspects of the variable volume pneumatic capacitance. Detailed investigations of steady state and transient conditions of charging and discharging processes of pneumatic capacitors were carried out by Zalmanzon [3,4]. Most of the analytical solutions were based on cases where isothermal flow

conditions were assumed. Experimental results were used to substantiate the theoretical work.

Letham [5], Kirshner [6], Woodson [7] and Humphrey and Manion [8] used electrical analogy to derive expressions for pneumatic capacitors. Caution must be exercised during application of the simplified equivalent electrical expressions for pneumatic capacitance because of the highly non-linear characteristics of real fluid flow which may result, in certain cases, in a significant departure from the exact electrical analogy. The volume flow approach was used by Hind and Hahn [9] in their attempt to develop the transfer funetion of the pneumatic capacitance of a fixed mass of gas enclosed in a rigid container. When certain simplifying assumptions were made, the transfer function was shown to be related solely to the polytropic index of compression.

Dagan [10] analysed the static and dynamic characteristics of fixed volume capacitors. Dritsas [11] recently analysed the variable volume capacitor's static and dynamic characteristics. Both studies were carried out purely from the basic thermodynamic and fluid mechanics point of view. The results, similar to those presented by Hind and Hahn, indicated that the process of

charging and discharging of pneumatic capacitors depends on the polytropic index "n". Extensive experimental results were presented by Dagan only to substantiate the theoretical work.

The present experimental study was undertaken to acquire a better insight into the actual charging and discharging mechanisms in variable pneumatic capacitors and to establish the true value of the polytropic index "n" which will be representative of the actual pneumatic circuit.

The main objectives of the present experimental study are defined as follows:

- Experimental investigation of the charging and discharging processes of the variable volume capacitors.

- Comparison of the experimental and theoretical results to determine the trend of variation of the proper polytropic index "n" of the processes when the spring constant of the bellows, the compressed air temperature and the room temperature are constant.

CHAPTER 2

EXPERIMENTAL INVESTIGATIONS

2.1 General

A pneumatic capacitor is a passive device which does not require a power supply but is capable of modulating input signals characteristic of the element. A variable volume pneumatic capacitor consists basically of a chamber with one or more input or output ports such as bellows or balloons as shown in Fig. 1. The type of variable volume capacitor investigated in this report is confined to the bellows type. The elastic properties of the bellows, the compressibility of the gas as well as the pressure variation due to heat transfer which affects the overall capacitance is also considered.

Consider the case with variable volume capacitor having an input and an output port. Fluid is first admitted through the input port during the charging process and at the same time, vented through the output port. When the input terminates and the discharging mode takes place, fluid will be vented through both input and output ports simultaneously. Therefore, in order for the pressure to build up within the capacitor, the inflow rate

must be greater than the outflow rate. A series of experiments were designed and carried out to record the pressure rise-time characteristics of variable volume capacitors. Results are compared with theoretical values to establish the proper polytropic index "n" for both the charging and discharging processes.

2.2 Apparatus

The apparatus used are summarized in Table I. All the flowmeters, transducers and measuring instruments were checked and calibrated according to the manufacturer's specifications.

2.3 Fluid Amplifier Characteristics

The fluid amplifiers used were supplied by Aviation Electric Ltd., the manufacturer. In order to verify the operational characteristics claimed by the manufacturer as shown in Appendix I, the following tests were conducted. The schematic diagrams of the test set-up are shown in Fig. 2.

2.3.1 Output Characteristics of Fluidic Monostable Amplifier 1100M01 (No. 1)

The pressure-flow characteristics were obtained for the charging amplifier (No. 1) output leg "01" which

is normally the active output port for the monostable amplifier and which is later used in the experiment to connect with the input of the capacitor. The test was repeated for six different supply pressures of 2.5, 5.0, 7.5, 10.0, 12.5 and 15.0 psig. A schematic of the experimental set-up is shown in Fig. 2a and the detailed procedure described in Appendix II. The output characteristics of AEL Monostable Amplifier AE 1100M01 are presented in Fig. 3.

2.3.2 "Reverse Flow" Characteristics of Monostable Amplifier AE 1100M01 (No. 1)

The reverse flow characteristics through "01" for six different supply pressures of 2.5, 5.0, 7.5, 10.0, 12.5 and 15.0 psig were obtained using test set-up as shown in Fig. 2b. The detailed procedure is described in Appendix II. The experimental results are shown in Fig. 4a, where the data is superimposed on the theoretical orifice flow curves plotted for different equivalent flow areas. The experimental results for the various supply pressures indicate that these are independent of the supply pressure of the amplifier.

2.3.3 "Load-Line" Pressure-Flow Characteristics of Monostable Amplifier AE 1100M01 (No. 2)

The load line characteristics of the amplifier were obtained using the schematic as shown in Fig. 2c with the detailed procedure described in Appendix VI, for six different amplifier supply pressures of 2.5, 5.0, 7.5, 10.0, 12.5 and 15.0 psig. The experimental results are shown in Fig. 4b. The load line characteristic, such as the reverse flow case, is independent of the supply pressure.

2.4 Experimental Set-Up

Studies were conducted on the charging and discharging behaviour of four variable volume pneumatic capacitors of the bellows type. The physical characteristics of the capacitors are shown on Tables II (a, b, c, d). The charging process was performed by connecting the output 01, which is normally active, of a monostable amplifier (Aviation Electric #1100M01) to the pneumatic capacitor input port as shown schematically in Fig. 5. The reason for using 01 output port rather than 02 is to eliminate the possible introduction of error due to the additional flow rate of the control input.

The ON-OFF switch which is connected parallel to the air supply is normally ON. Turning the switch to its OFF position, the control jet supply pressure is OFF and the output of the amplifier switches immediately from 02 to 01. Charging of the variable capacitor takes place. The upper control port C1 of another identical monostable amplifier operating at the same supply pressure as that of the charging amplifier is connected to the pneumatic capacitor output port. Every capacitor was charged and discharged by the amplifiers with supply pressures of 2.5, 5.0, 7.5, 10.0, 12.5 and 15.0 psig. The pressure variations within the capacitor were monitored by a Validyne pressure transducer, Model No. DP15TL. Since the transducer's cavity volume was extremely small (less than 0.05% of the smallest chamber considered), its effect for practical purposes was neglibible.

The output of the transducer was fed to a transducer indicator-amplifier made by Validyne, Model No.CD12. The amplifier's output was fed to a Gould, Model No. 11-6402-05 strip chart recorder with chart drive speed of 25 mm/sec. Static calibration of the transducer and amplifier was carried out according to the procedure recommended by the manufacturer. Results of the calibration are shown in Fig. 6.

CHAPTER 3

RESULTS AND DISCUSSIONS

3.1 Presentation of Results

A strip chart recorder was used to record the charging and discharging characteristics of the tested variable volume capacitors. The experimental results at different values of supply pressures are accurately reproduced and presented in the same graph as the theoretical pressure rise and drop rates for the charging and discharging variable volume capacitors obtained from V. Dritsas' Major Technical Report [11] by solving the differential equations. The constants required to obtain these analytical solutions were established from the experimental curves shown in Figs. 3, 4a and 4b. In addition, the initial pressure condition of the capacitor is the ambient pressure.

The analytical solutions represent the two extreme cases of the charging and discharging process: the adiabatic case where the polytropic index is equal to 1.4 and the isothermal case where the polytropic index is equal to 1.0. The actual processes will lie somewhere between these two extreme cases.

The volume of the experimental chambers varies with changes in the supply pressure. According to the manufacturer's specification, the maximum pressure supplied to the bellows was limited to I5 psig. Typical graphs of supply pressure versus length change for bellows No. 3 and 4 are shown in Figs 7 and 8 respectively.* However, due to some plastic deformation taking place between experiments, the results are not as consistant as originally expected. The experiments were conducted using four different variable capacitors Nos. I, 2, 3 and 4 with free length volumes of 36.6 in^3, I8.5 in^3, 6.3 in^3 and I.I in^3 respectively. The results are grouped as follows:

Capacitor size No. I (Figs. 9 to I4)
Capacitor size No. 2 (Figs. I5 to 20)
Capacitor size No. 3 (Figs. 2I to 26)
Capacitor size No. 4 (Figs. 27 to 32)

3.2 Discussion of Results

By comparing the results for each variable volume chamber, it can be seen that the rate of pressure rise and drop is basically a function of the supply pres-

*Determination of the spring constant K is discussed in Appendix III.

sure and the change in volume. The lower the supply pressure, the smaller the change in volume and the faster the resultant pressure rise (or drop) takes place. At low pressures, the spring force of the capacitor is higher than that resulting from the supply pressure and therefore, small changes in volume occur. At high pressures, however, the supply pressure force overcomes the spring force and large changes in the chamber volume take place. It is suspected that the pressure time characteristics during charging and discharging are also dependent to a certain extent on the diameter to length ratio of the capacitor.

The experimental and theoretical results for capacitor size No. 1 are shown in Figs. 9 to 14. At 2.5, 5.0 and 7.5 psig, the actual process follows very closely the theoretical adiabatic process until the pressure rises to about 30-35% of its maximum value. It then deviates from the adiabatic process and rapidly approaches the isothermal case. At the higher supply pressures of 10.0, 12.5 and 15.0 psig, the actual process closely follows the adiabatic process during the initial part of charging, but at these supply pressures, the actual process begins to depart towards the isothermal process in the vicinity of 35-45% of the maximum pressure. This finding indicates

that the rate of pressure build-up within the capacitor is quite rapid during the initial stage of charging because the inflowing air has gone through a rapid expansion process with a finite temperature drop. However, there is not enough time for heat transfer to take place. As a result, the process approximates the adiabatic one with the polytropic index equal to 1.4. As the rate of charging is decreased, it can be seen from the graphs, that sufficient time is allowed for heat transfer to take place even though the chamber volume changes very little. The process gradually falls closer to that of an isothermal case where the polytropic index equals 1.0.

It is evident from the graphs that in the initial period of the discharge process, both the theoretical, isothermal and adiabatic processes at different supply pressure conditions are very close to each other. Experimental results of the actual discharging falls within the two extreme theoretical uses. In general, the actual process tends to be closer to the isothermal especially in the final phase of discharging. The discharging process starts when the pneumatic chamber has reached its maximum pressure for a given supply pressure. Since sufficient time has elapsed and due to heat transfer, the temperature of the accumulated air in the capacitor is

nearly the same as that of the ambient. Consequently, the theoretical curves for the adiabatic and isothermal cases are very close. However, it is advisable that the isothermal case be used for prediction of the discharge characteristics.

The experimental and theoretical results for capacitor No. 2 are shown in Figs. 15 to 20. At 2.5 and 5.0 psig, the actual process again follows very closely the theoretical adiabatic until the pressure rises to about 50% of its maximum value. It then deviates from the adiabatic and gradually approaches the isothermal process and at 75% it meets the theoretical isothermal process. At 7.5 and 10.0 psig supply pressure, the experimental process lies equally between the adiabatic and isothermal curves. For higher supply pressures of 12.5 and 15.0 psig, the actual process follows the adiabatic until the output pressure rises to about 60% of its maximum value, then quickly approaches the isothermal which meets at 80% of the output pressure value.

From the above observation it seems that at the initial stages of the charging process, air enters the capacitor and expands rapidly and there is not sufficient time for significant heat transfer to take place. As a

result, the process resembles the adiabatic. As the pressure starts to build, the spring of the bellows tends to oppose any change in chamber length. At this stage, the time intervals involved are greater and heat transfer does take place. Hence, the actual process moves from adiabatic to isothermal. The discharging process at any of the supply pressures, with the exception of the 12.5 psig supply pressure, exhibits the same behaviour with capacitor No. 1 as described previously. The discharging process at a supply pressure of 12.5 psig, as shown in Fig. 19, provides some discrepancy which is probably due to some experimental errors.

The experimental and theoretical results for capacitor size No. 3 are shown in Figs. 21 to 26. At all supply pressures, the actual process follows very closely to the theoretical adiabatic process until the pressure output rises to about 60% of its maximum value, then slowly deviates from the adiabatic and quickly approaches the theoretical isothermal process. The experimental curves cross the isothermal curve at approximately 80% of the maximum output pressure. The actual discharge process adheres closely to the adiabatic and isothermal. From the graphs, it is apparent that the actual process adheres closer to the isothermal and for all practical purposes,

the isothermal index n=1.0 can be used without any appreciable errors. Since the charging and discharging phenomenon for size No. 3 capacitor is very similar to the cases previously discussed, no further explanation is considered necessary in this case.

The experimental and theoretical results for capacitor No. 4 are shown in Figs. 27 to 32. At the amplifier supply pressures of 2.5, 5.0, 7.5, 10.0, 12.5 and 15.0 psig, the actual process again follows very closely to the theoretical adiabatic process, until the pressure in the capacitor rises to about 65-75% of its maximum value. Then the actual process begins to shift closer to the isothermal process and cut the isothermal wire at approximately 80-85% of the maximum output pressure level. The rate of charging decreases with increasing pressure within the capacitors. Hence, sufficient time is allowed for the heat transfer to take place and therefore, at the final phase, the charging process resembles that of an isothermal case where the polytropic index is equal to 1.0.

During the discharge process, at any of the supply pressure conditions, both the theoretical isothermal and adiabatic processes follow very closely to the

actual processes. At the final phase of the discharging process, the actual process moves rapidly towards the adiabatic and then reverts back to the isothermal. This may be attributed to the elastic properties of the material. Since discharging commences when the pneumatic chamber has reached its maximum pressure, sufficient time has elapsed for heat transfer to take place and the temperature of the experimental chamber is nearly equal to the ambient. The discharging process can again be better represented by the theoretical isothermal process.

In control system circuits where capacitors are used to create time delay for building up pressure levels, the desired pressure level is usually below 63.2% of the maximum attainable level of the chamber. If the operation of the time delay circuit is confined within the region where a well defined pressure-time characteristic is repeatedly obtainable, it follows from the results that the adiabatic process may be considered for predicting charging processes at capacitors with mean diameter to free length ratios of $.8 \leq \frac{D_m}{L_o} \leq 1.7$ for practical circuit design. Both the theoretical adiabatic and isothermal processes may be used to predict discharging processes of capacitors of mean diameter to free length ratios of $.8 \leq \frac{D_m}{L_o} \leq 1.7$ without introducing appreciable error.

As can be seen from the curves 9 to 32 for all capacitors tested, the actual charging curves never reach the level of the theoretical isothermal and adiabatic process curves. This can be partially attributed to insufficient time allowed for the charging. Furthermore, assumptions made in deriving the theoretical model were frictionless flow and ideal gas equation. Also, no geometric effect of the capacitor was considered. It is believed that such effects may be significant.

To better understand the charging and discharging phenomena, the "time constant" will be used for comparison between the various results. The time constant for charging of capacitors is defined as the time required to charge the capacitor up to 63.2% of its maximum capacity. Similarly, for the discharging of the capacitors, the time constant is defined as the time required for pressure to drop to 36.8% of the capacitor's maximum pressure level. All the time constants obtained for charging and discharging are tabulated in Tables III to VI. It can be seen from Tables III to VI that the time constant increases as the supply pressure increases. It must be also pointed out that as the supply increases, the final volume of the capacitor also increases. The increase in volume depends on the spring constant of the

specimens which in turn, is a function of the supply pressure. This increase in time constant is expected because both the charging amplifier and discharging equivalent area are kept constant. Therefore, since the volume increases, more time is required to complete the charging process. Similarly, the time constant for the discharge process is higher at the higher supply pressures. This is evident from the fact that the volume is larger at higher pressures. The discharging process time constants are approximately 60% of those of the charging process.

From Table V it can be seen that the charging time constant increases with increasing pressure. Even though the free volumes of the two specimens are quite different (6.3 in^3 and 1.1 in^3), the time constants are about the same. Similarly, for the discharging process of the capacitor, the time constant increases with higher supply pressure values. These results may be traced back to experimental errors. However, it must be noted that the increase in the time constant at different supply pressures is not necessarily a linear relationship. For example, an increase of 100% in the supply pressure from 7.5 psig to 15.0 psig causes an average increase in time constant of less than 40%. This means that for high supply pressures, the pressure rise rate (or drop) in the capacitor is

actually faster than at low supply pressures.

Below the pressure value of the time constant (63.2%), a linear pressure-time relation can generally be used for consideration of charging. This result and the interrelationships between time constants, amplifier supply pressure and bellows volumes can be most useful for the design of fluidic amplifier systems and circuits.

It should be noted that all experimental results of the present study were obtained on a particular test set-up and under specific environmental conditions, i.e. 70°F room temperature and 14.6 psia pressure.

CONCLUSIONS

Experimental investigations of the charging and discharging of variable volume capacitors in conjunction with the operating characteristics of a fluid amplifier were carried out. The true polytropic index of the actual charging and discharging processes can be established by comparing the theoretical curves calculated from the analytical models for different values of the polytropic index with experimental data.

The results generally indicate that for the charging of the pneumatic capacitors, the adiabatic process of n=1.4 can be used up to a pressure level of 50% of the maximum with the isothermal where n=1.0 from that point on. Furthermore, for the discharging process, both the theoretical adiabatic and isothermal processes may be used. However, it is advisable that the isothermal case be used for the prediction of the discharge characteristics.

The technique developed for predicting the true charging and discharging processes of variable volume pneumatic capacitors in conjunction with known fluid amplifier performance characteristics can be used in the Engineering design of time-delay and oscillation circuits.

REFERENCES

1. Ahrendt, W.R. and Taplin, J.R., "Automatic Feedback Control". McGraw-Hill, New York (1951) pp. 271-273.

2. Helm, L., "Determination of Pneumatic Capacities of Variable Volume". Acta Technica (Budapest), Vol. 22 (1958) pp. 53-60.

3. Zalmanzon, L.A., "Components for Pneumatic Control Instruments". Pergamon Press, London (1965).

4. Zalmanzon, L.A., "Fundamentals of Theory and Design of Elements of Pneumo-Automatics" - published in "Pneumatic Components and Computing Devices for Control Systems". Butterworths, London (1963).

5. Letham, D.L., "Fluidic System Design". Machine Design, Penton Publications, Vol. 38, 7 (1966) pp. 170-181.

6. Kirshner, J.M., "Fluid Amplifiers". McGraw-Hill Book Co., New York (1966) pp. 146-186.

7. Woodson, C.W., "AC Fluidics". Western Electronic Show and Convention, Los Angeles, California, August 1968.

8. Humphrey, R.L. and Manion, F.M., "Low-Pass Filters for Pneumatic Amplifiers". Proc. of the Fluid Amplification Symposium, Vol. 1, Harry Diamond Laboratories, Washington, D.C., May 1964.

9. Hind, E.C. and Hahn, E.J., "The Transfer Function of the Pneumatic Capacitance". ASME Paper 65-WA/AUT-18 (1965).

10. Dagan, J., "Study of Pneumatic Capacitors". A Dissertation, Sir George Williams University (1971).

11. Dritsas, V., "A Theoretical Study of Variable Volume Capacitors". Technical Report, Sir George Williams University (1975).

12. Zalmanzon, L.A., "Components for Pneumatic Control Instruments". Pergamon Press, London (1965).

13. Doebelin, Ernest O., "Measurement Systems: Application and Design".

14. Shearer, J.L., Murphy, A.T. and Richardson, H.H., "Introduction to System Dynamics".

TABLE I

Apparatus	Manufacturer	Model No.	Serial No.
Pressure Transducer	Validyne Engineering Corp.	DP15TL	18222
Transducer Indicator Amplifier	Validyne Engineering Corp.	CD12	11197
Flow Meter	Fisher & Porter Co.	10A3500	C-1420-TA-A
Strip Chart Recorder	Gould Inc. Instrument Systems Division	11-6402-05	00377
Monostable Amplifier	Aviation Electric Limited	1100M01	-
Variable Resistor	Whitey Inc.	01RF2/1RF2	-
Pressure Regulator	Moore Instrument Company	Nullmatic 40-15	PC-1321
Pressure Gauges	U.S. Gage Company	0-15 psi 0-50 psi	- -

TABLE II(a)

BELLOWS PHYSICAL CHARACTERISTICS

CAPACITOR SIZE No. 1

INSIDE DIAMETER (I.D.) IN	OUTSIDE DIAMETER (O.D.) IN	MEAN DIAMETER (D.M.) IN	FREE LENGTH (Lo) IN	EQUIV-ALENT AREA (AE) IN^2	FREE LENGTH VOLUME (Vo) IN^3	RATIO DM/Lo
3.8	4.7	4.3	2.6	14.5	36.6	1.7

TABLE II(b)

CAPACITOR SIZE No. 2

INSIDE DIAMETER (I.D.) IN	OUTSIDE DIAMETER (O.D.) IN	MEAN DIAMETER (D.M.) IN	FREE LENGTH (Lo) IN	EQUIV-ALENT AREA (AE) IN^2	FREE LENGTH VOLUME (Vo) IN^3	DM/Lo
2.7	3.7	3.2	2.3	7.9	18.5	1.4

NOTE: ALL THE CHAMBERS USED ARE BRASS ALLOY MATERIAL, MANUFACTURED BY JOHNSON SERVICE COMPANY, MILWAUKEE WISCONSIN.

TABLE II(c)

BELLOWS PHYSICAL CHARACTERISTICS

CAPACITOR SIZE No. 3

INSIDE DIAMETER (I.D.) IN	OUTSIDE DIAMETER (O.D.) IN	MEAN DIAMETER (D.M.) IN	FREE LENGTH (Lo) IN	EQUIV-ALENT AREA (AE) IN^2	FREE LENGTH VOLUME (Vo) IN^3	RATIO DM/Lo
1.8	2.4	2.1	1.8	3.4	6.3	1.2

TABLE II(d)

CAPACITOR SIZE No. 4

INSIDE DIAMETER (I.D.) IN	OUTSIDE DIAMETER (O.D.) IN	MEAN DIAMETER (D.M.) IN	FREE LENGTH (Lo) IN	EQUIV-ALENT AREA (AE) IN^2	FREE LENGTH VOLUME (Vo) IN^3	DM/Lo
.9	1.3	1.1	1.2	.3	1.1	.8

NOTE: ALL THE CHAMBERS USED ARE BRASS ALLOY MATERIAL, MANUFACTURED BY JOHNSON SERVICE COMPANY, MILWAUKEE WISCONSIN.

TABLE III

TIME CONSTANTS

Charging: Measured Time Constants in Seconds as a Function of Supply Pressure.

P supply psig	Capacitor size No.1 Time Constants (secs)	Capacitor size No.2 Time Constants (secs)
2.5	.9	.5
5.0	1.5	.7
7.5	1.7	.7
10.0	1.7	.7
12.5	1.8	.8
15.0	1.8	.9

TABLE IV

TIME CONSTANTS

Discharging: Measured Time Constants in Seconds as a Function of Supply Pressure.

P supply psig	Capacitor size No.1 Time Constants (secs)	Capacitor size No.2 Time Constants (secs)
2.5	.7	.2
5.0	.8	.3
7.5	.9	.3
10.0	.9	.4
12.5	1.1	.4
15.0	1.1	.6

TABLE V

TIME CONSTANTS

Charging: Measured Time Constants in Seconds as a Function of Supply Pressure.

P supply psig	Capacitor size No.3 Time Constants (secs)	Capacitor size No.4 Time Constants (secs)
2.5	.2	.2
5.0	.2	.2
7.5	.2	.2
10.0	.2	.2
12.5	.3	.2
15.0	.3	.3

TABLE VI

TIME CONSTANTS

Discharging: Measured Time Constants in Seconds as a Function of Supply Pressure.

P supply psig	Capacitor size No.3 Time Constants (secs)	Capacitor size No.4 Time Constants (secs)
2.5	.1	.1
5.0	.1	.1
7.5	.1	.1
10.0	.2	.1
12.5	.2	.2
15.0	.2	.2

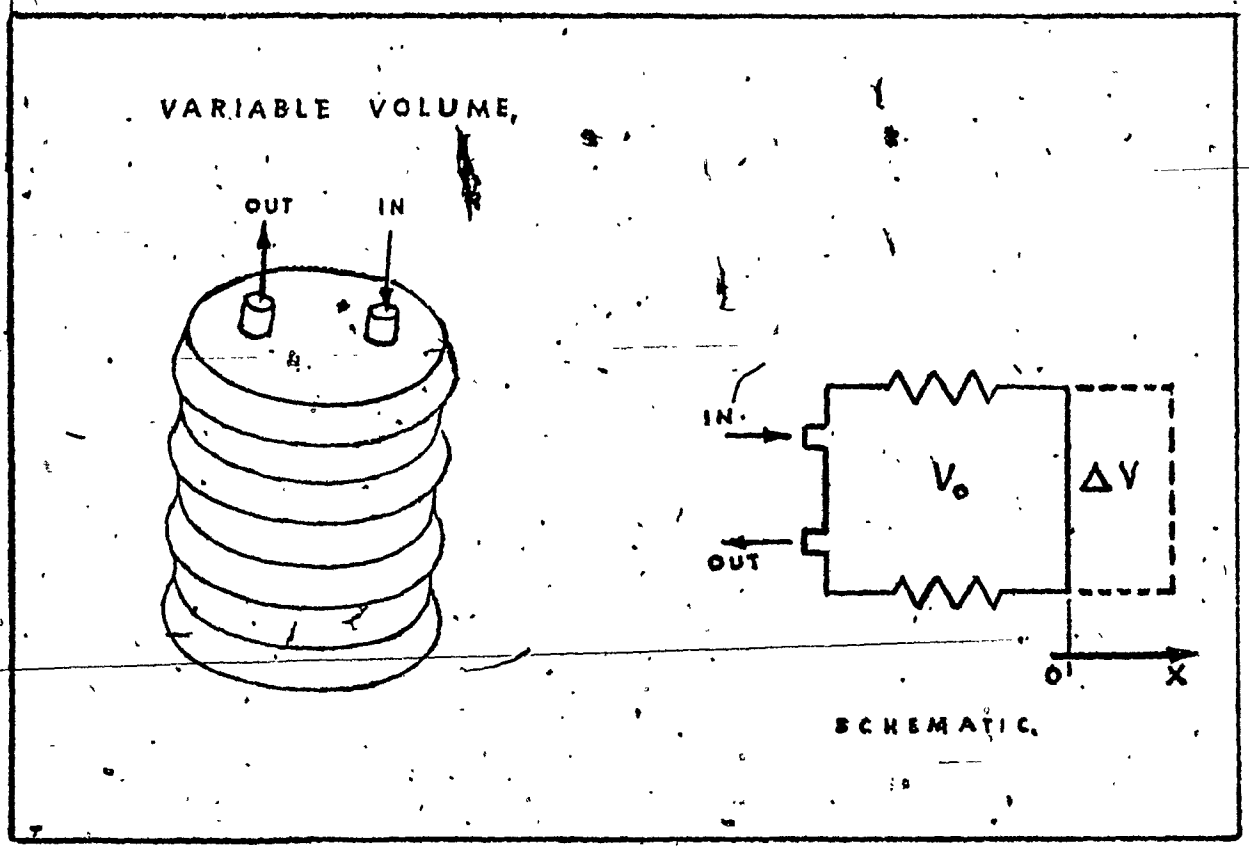

Figure 1. PNEUMATIC CAPACITORS.

(a) EVALUATION OF OUTPUT CHARACTERISTICS.

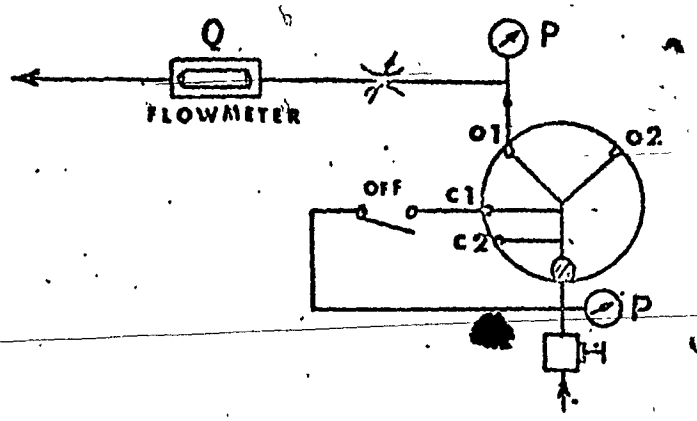

(b) VALUATION OF REVERSE FLOW CHARACTERISTICS.

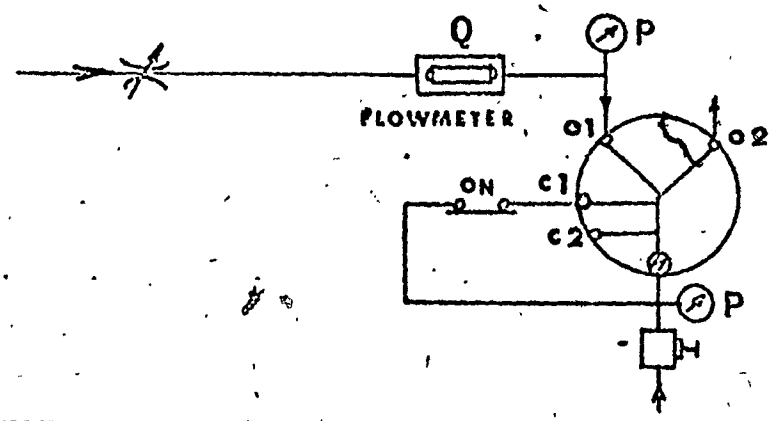

(c) EVALUATION OF LOAD-LINE CHARACTERISTICS.

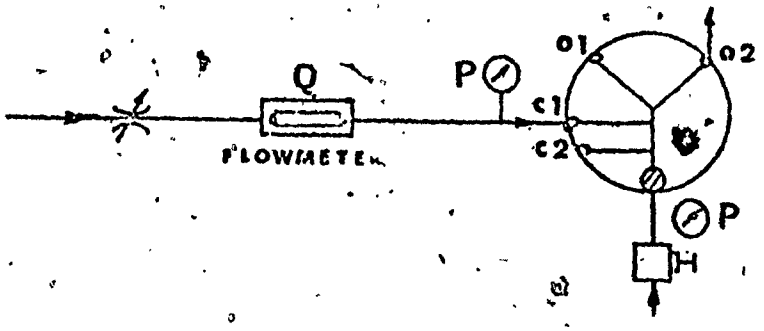

Figure 2 TEST SET UPS.

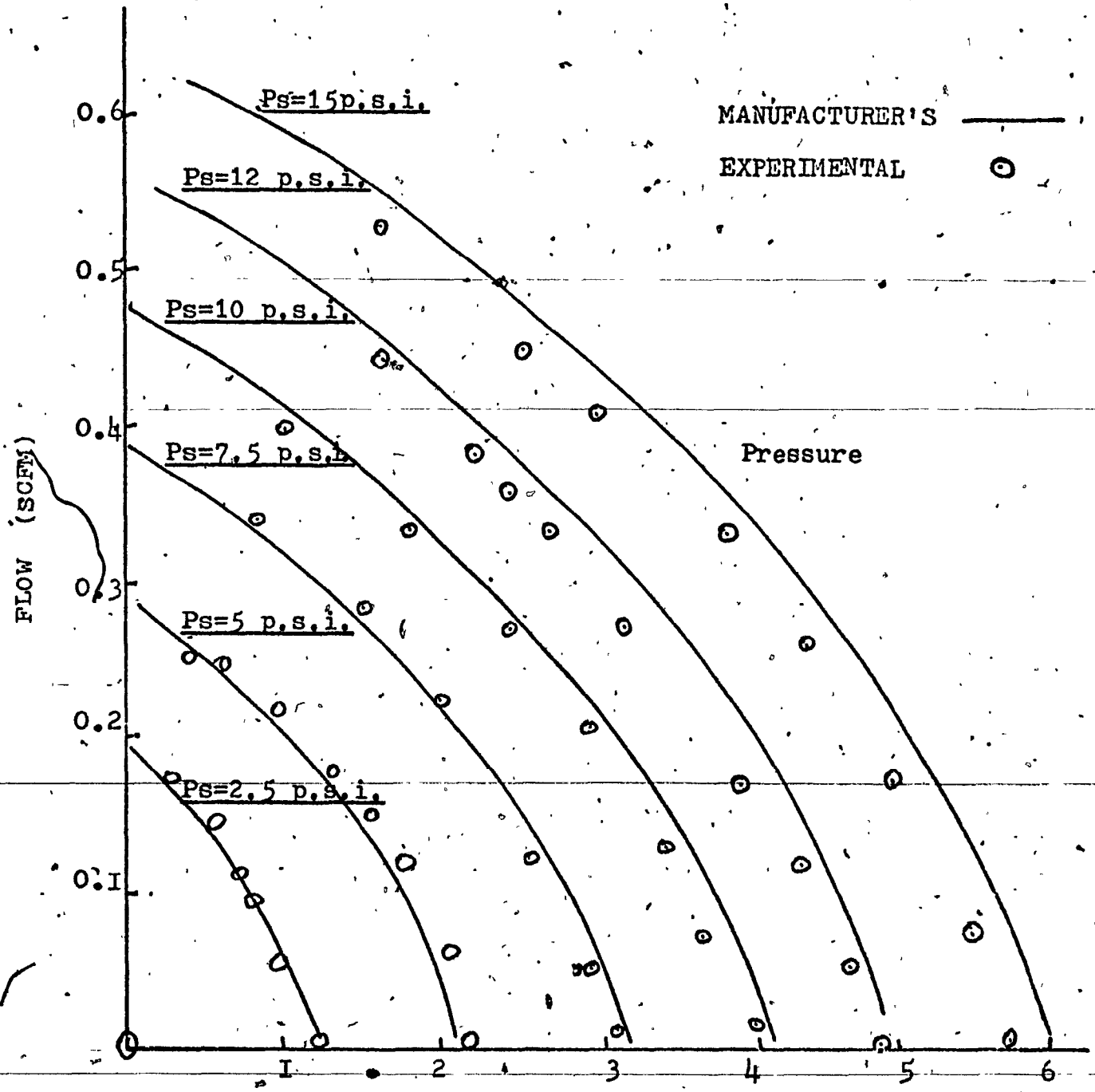

Figure 3 FLUID AMPLIFIER NO. AE 1100M01
OUTPUT CHARACTERISTICS

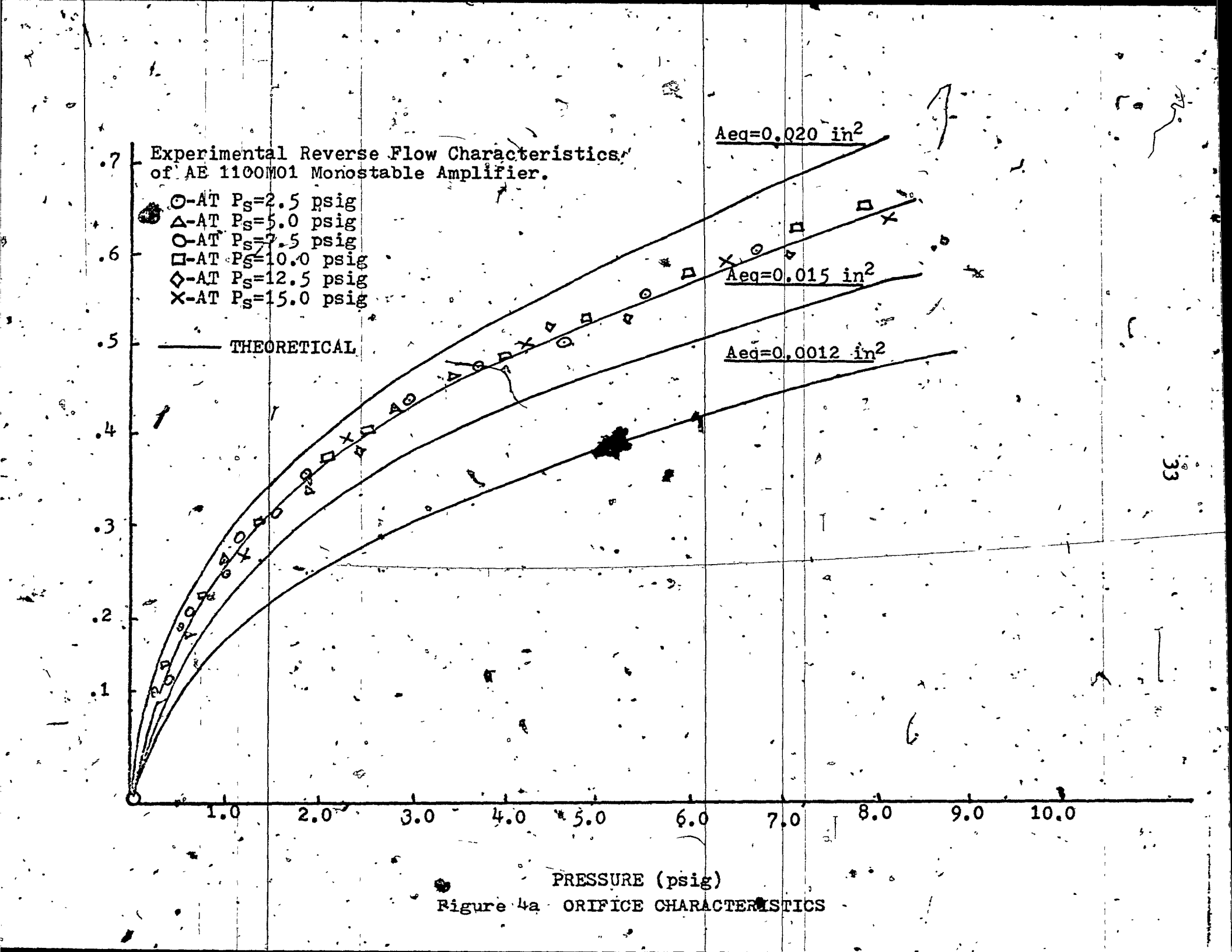

Figure 4a ORIFICE CHARACTERISTICS

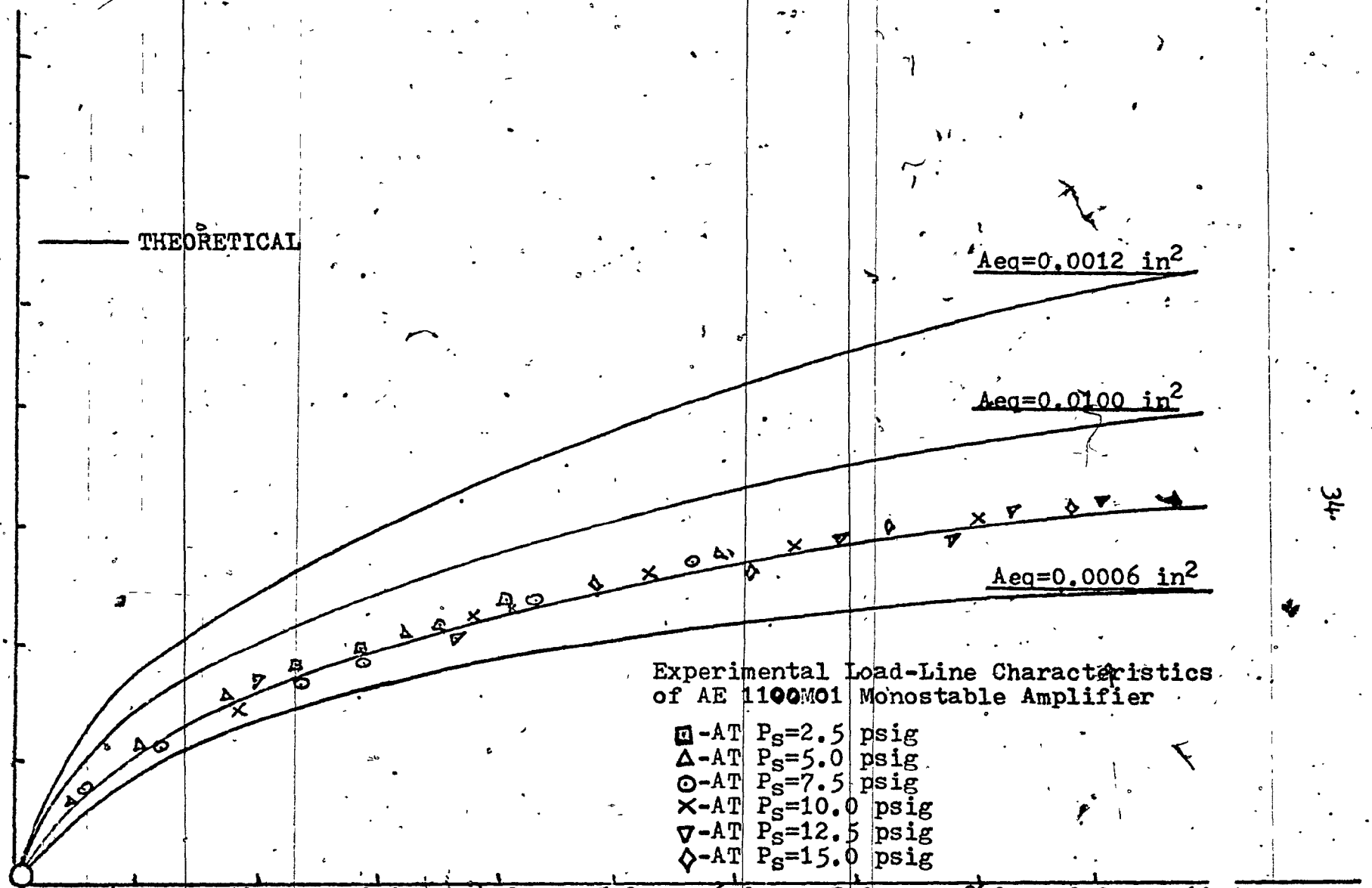

Figure 4b ORIFICE CHARACTERISTICS

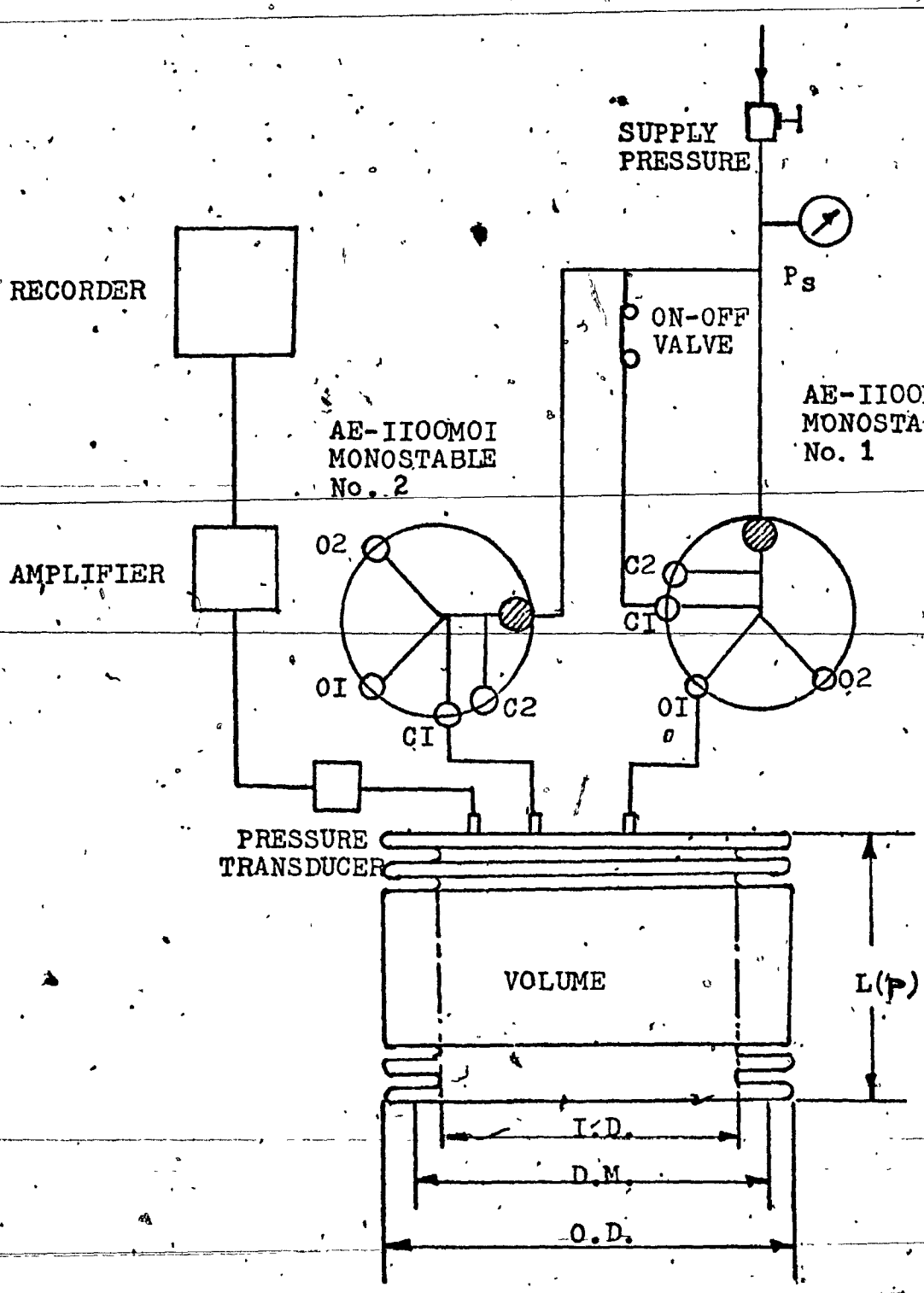

Figure 5 SCHEMATIC OF EXPERIMENTAL SET UP.

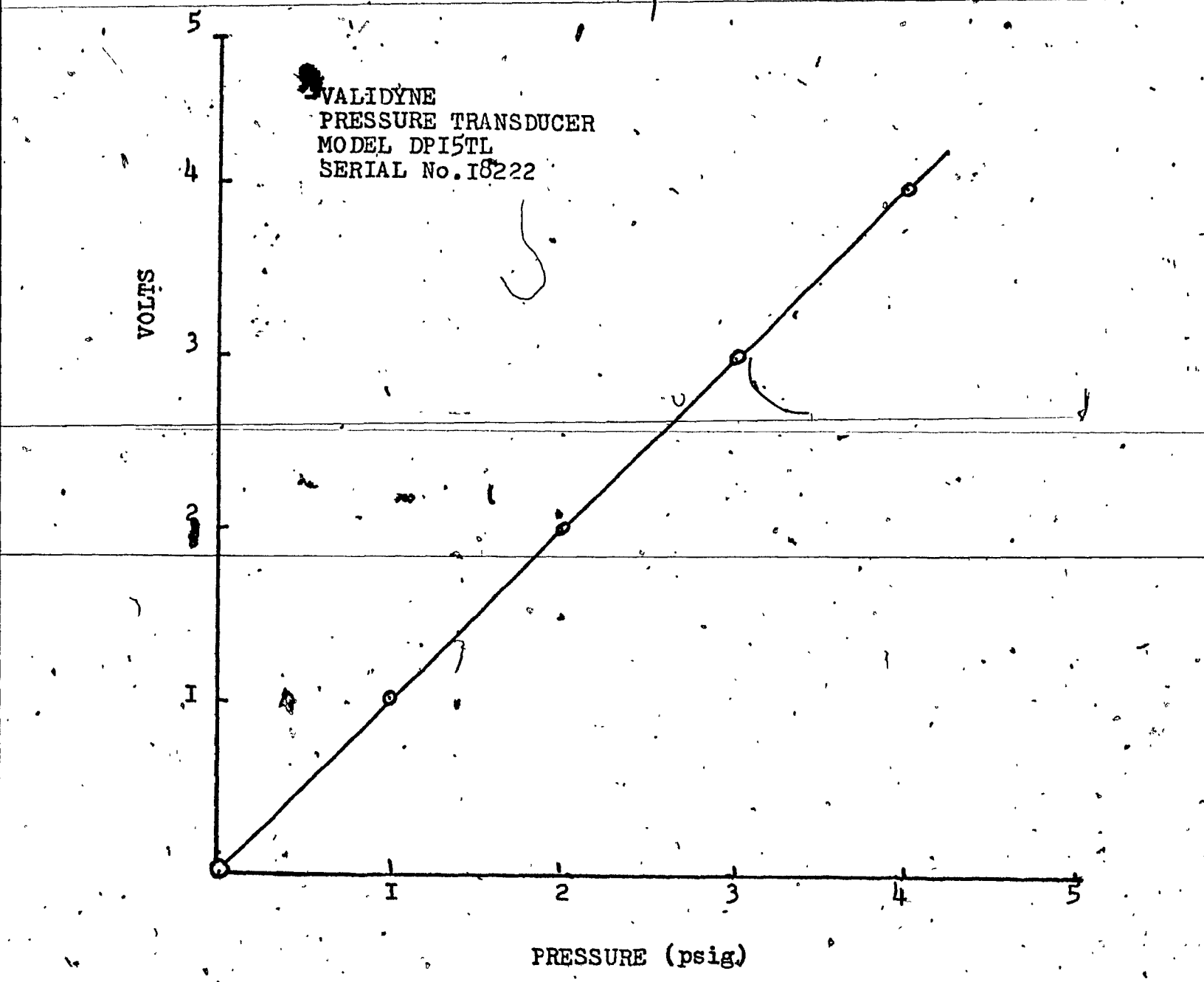

Figure 6 CALIBRATION OF PRESSURE TRANSDUCER

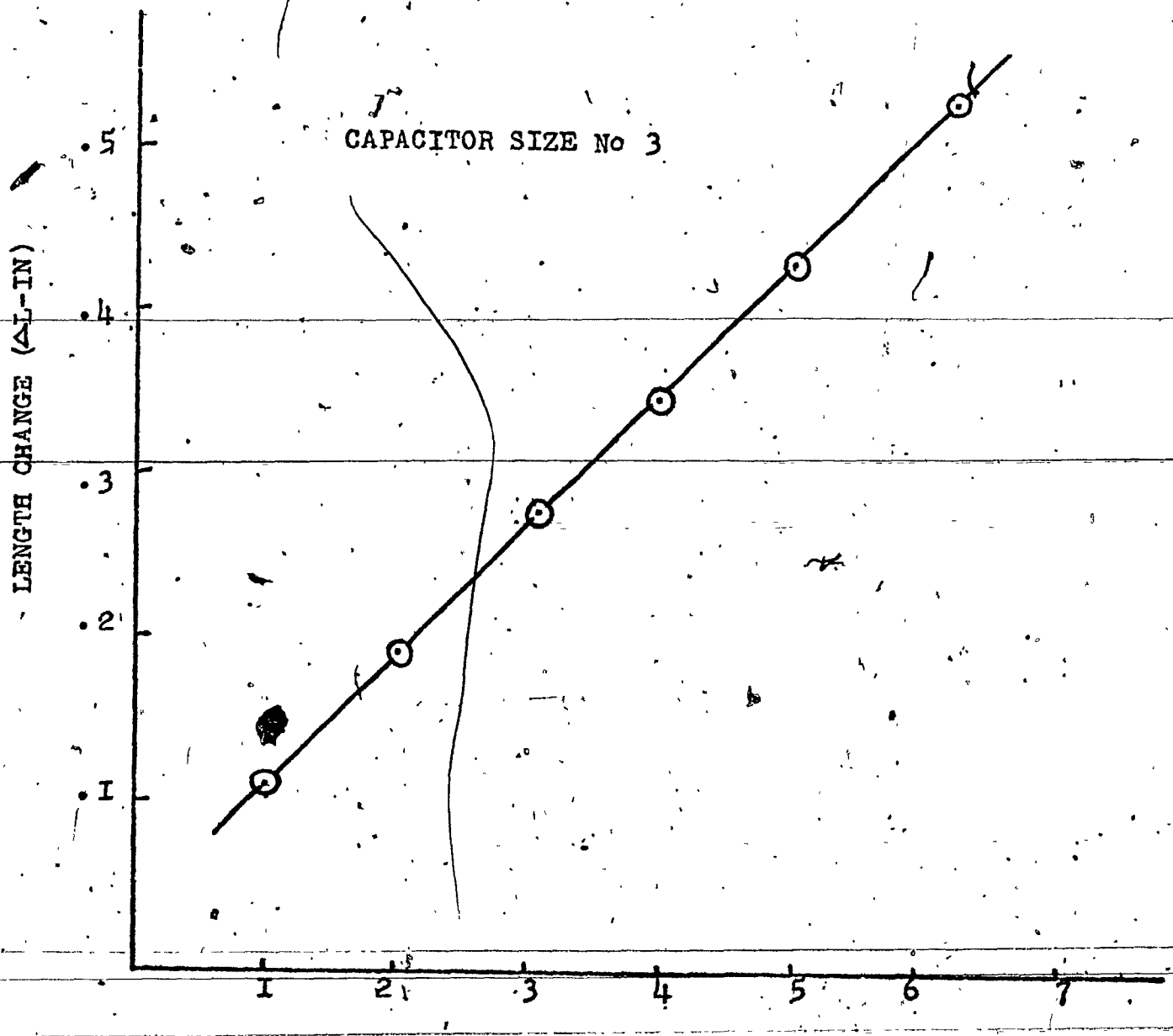

Figure 7 CHANGE OF LENGTH WITH PRESSURE

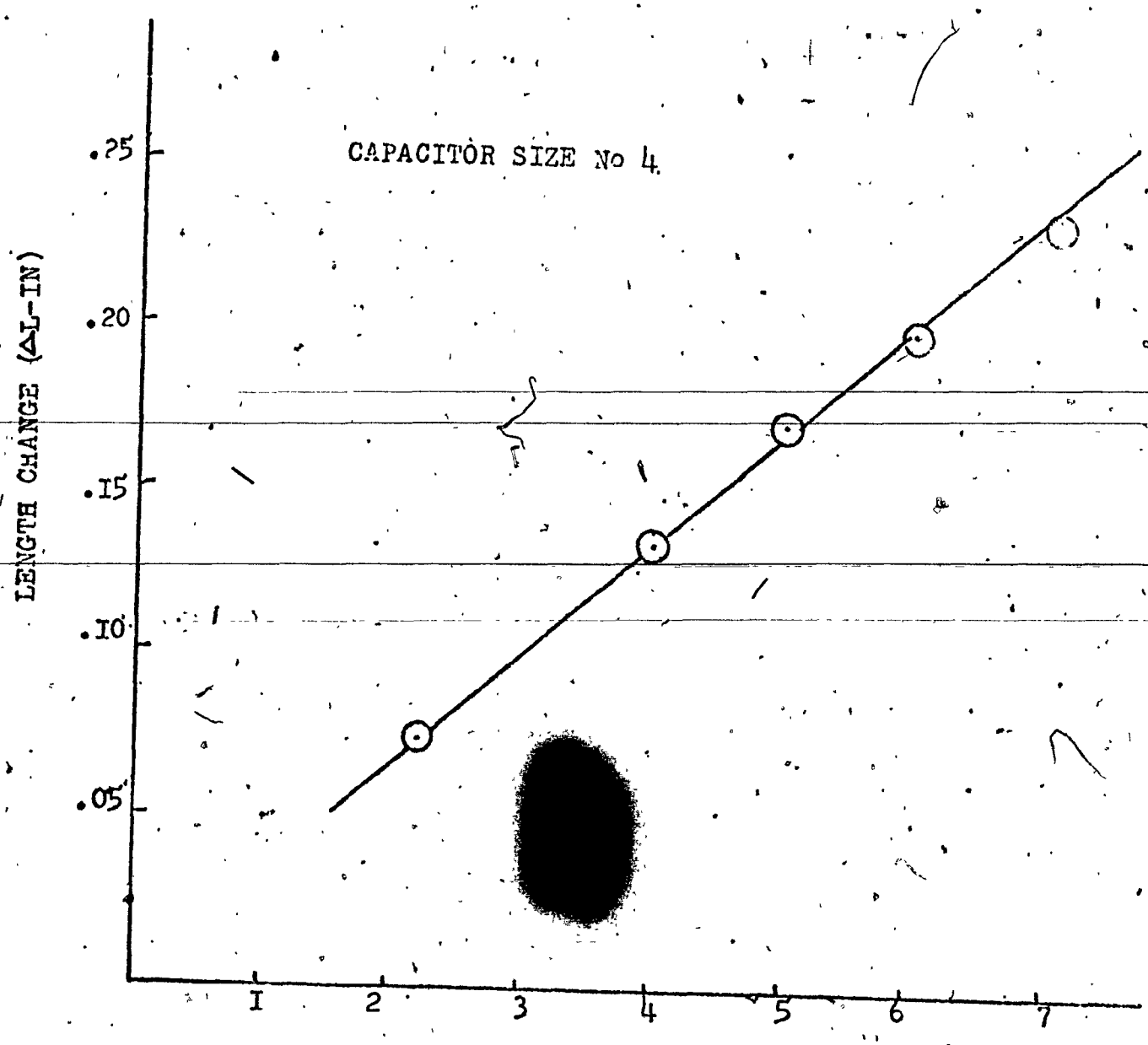

Figure 8 CHANGE OF LENGTH WITH PRESSURE

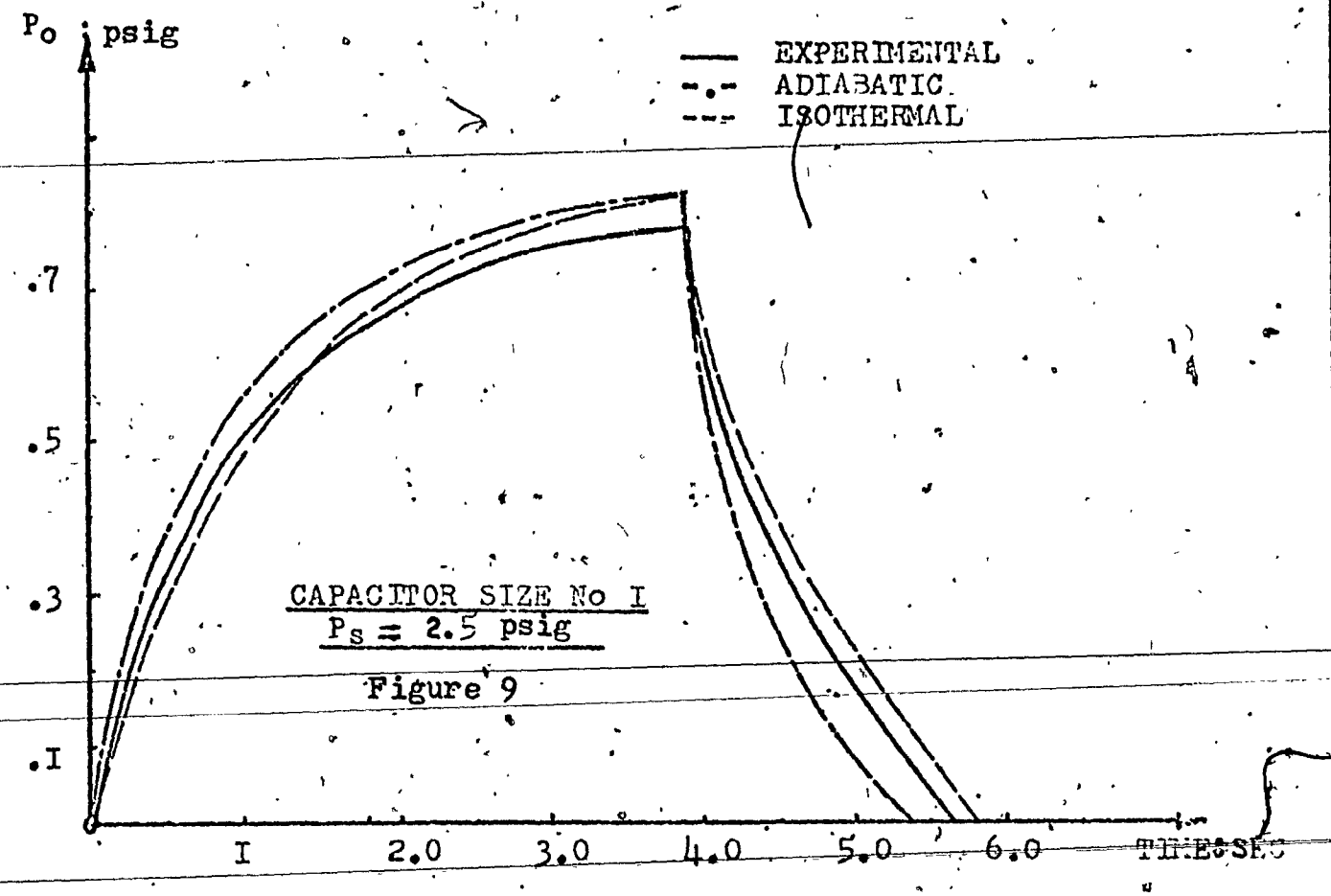

CAPACITOR SIZE No I
P_s = 2.5 psig

Figure 9

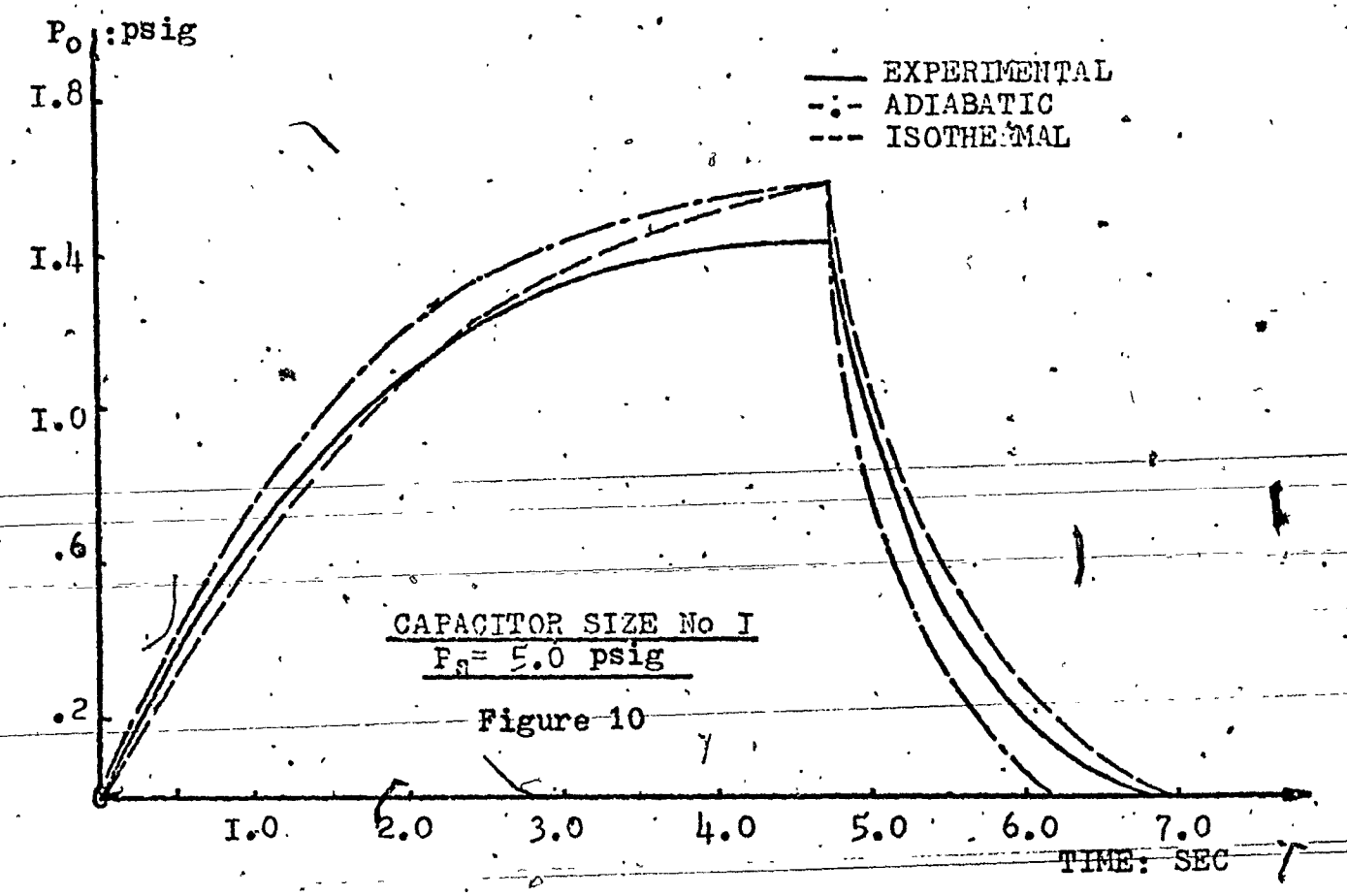

CAPACITOR SIZE No I
P_s = 5.0 psig

Figure 10

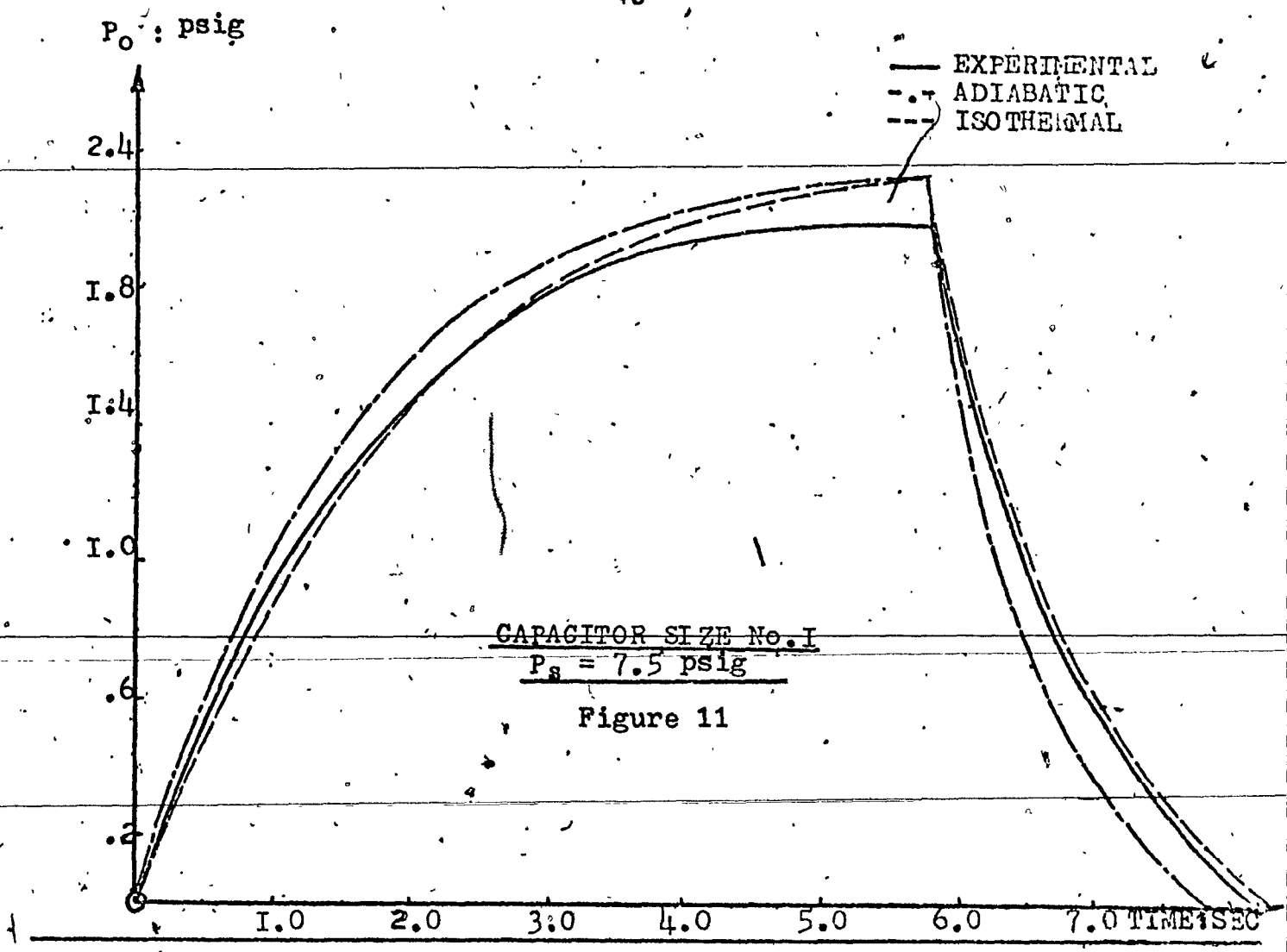

CAPACITOR SIZE No. I
P_s = 7.5 psig

Figure 11

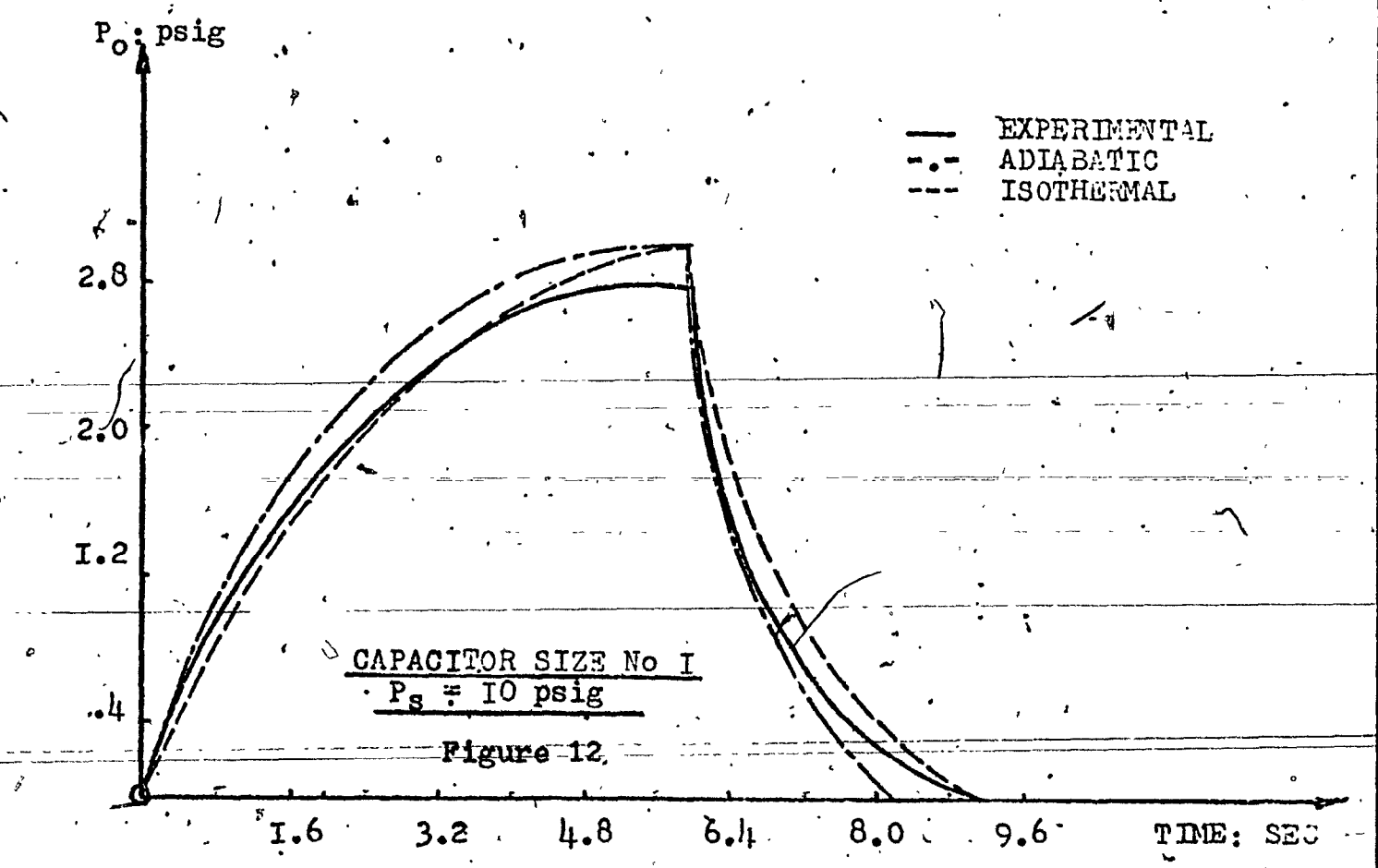

CAPACITOR SIZE No I
P_s = IO psig

Figure 12

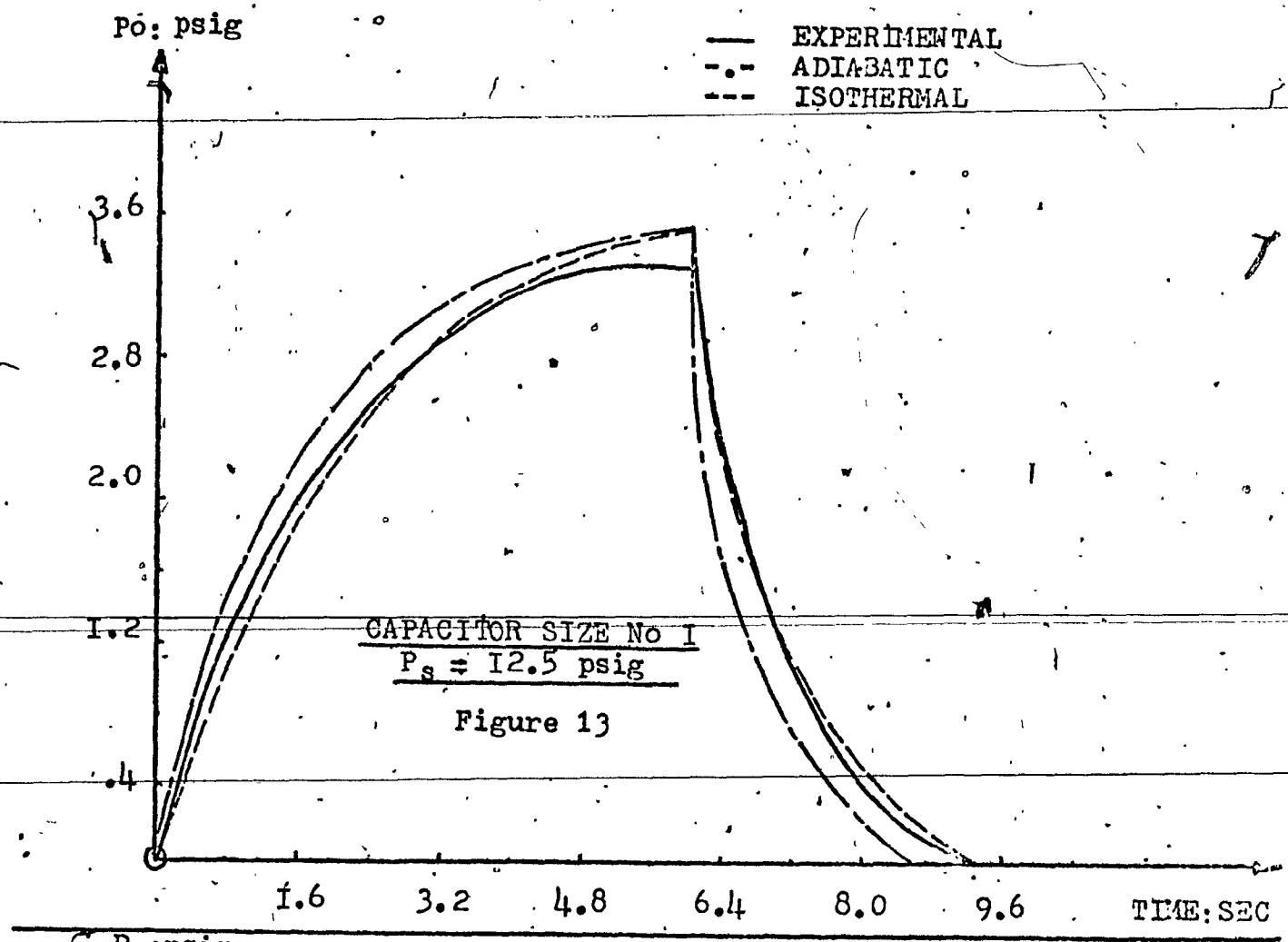

CAPACITOR SIZE No I
P_s = 12.5 psig

Figure 13

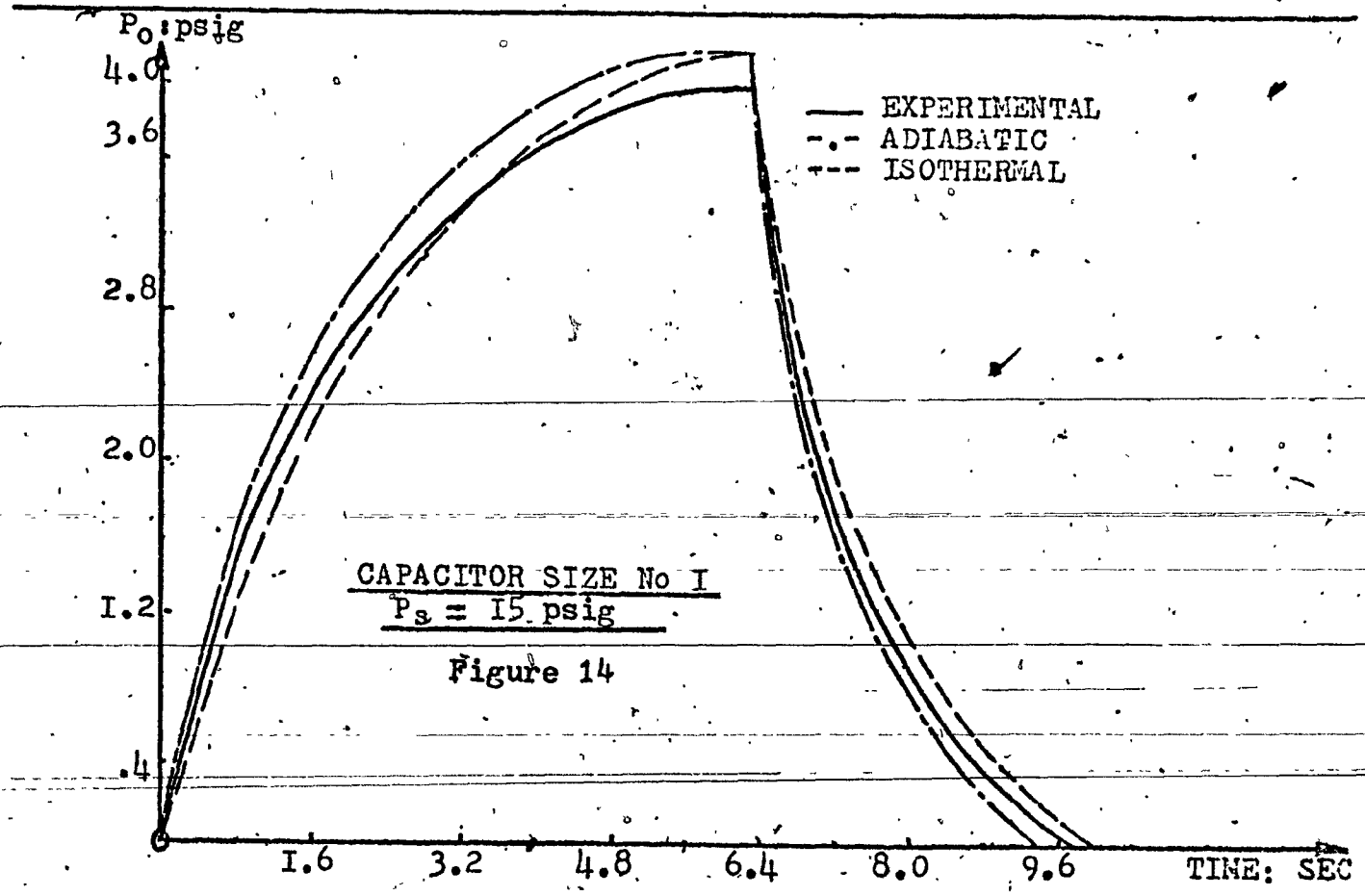

CAPACITOR SIZE No I
P_s = 15 psig

Figure 14

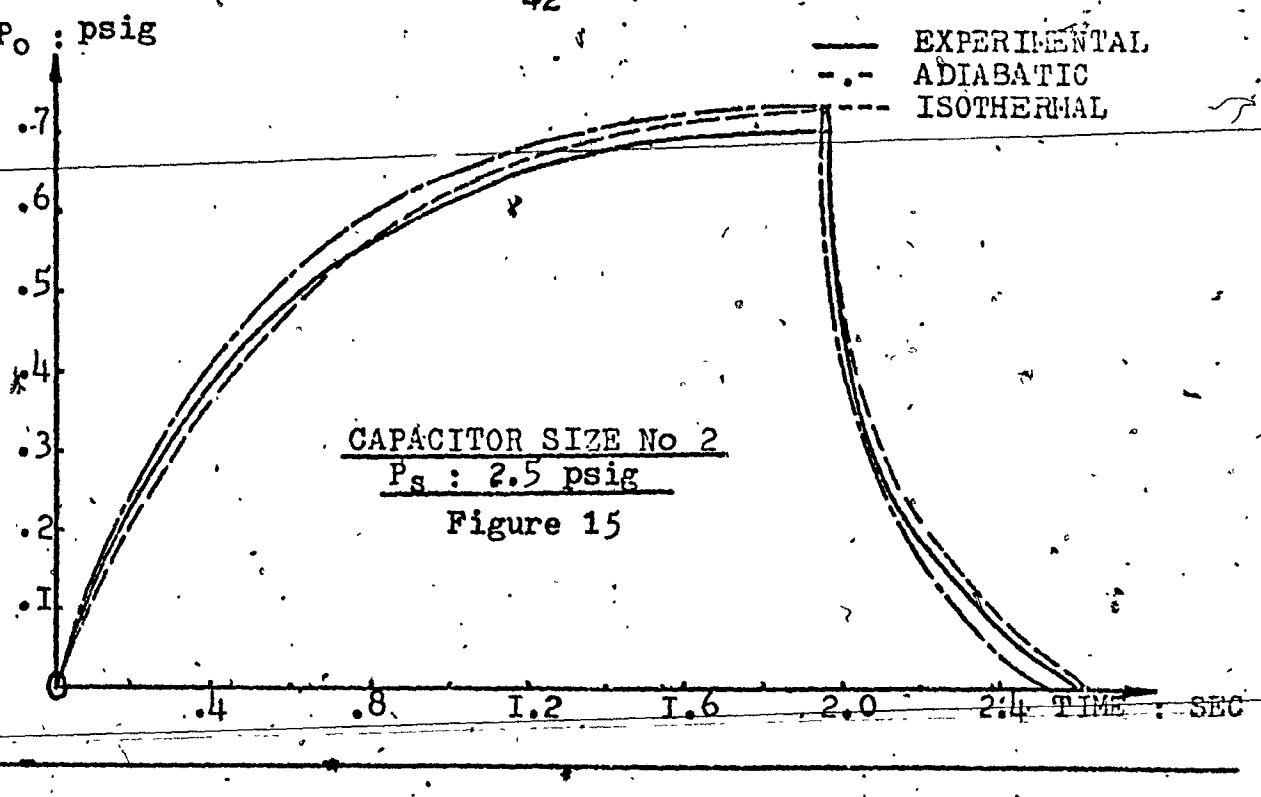

CAPACITOR SIZE No 2
P_s : 2.5 psig

Figure 15

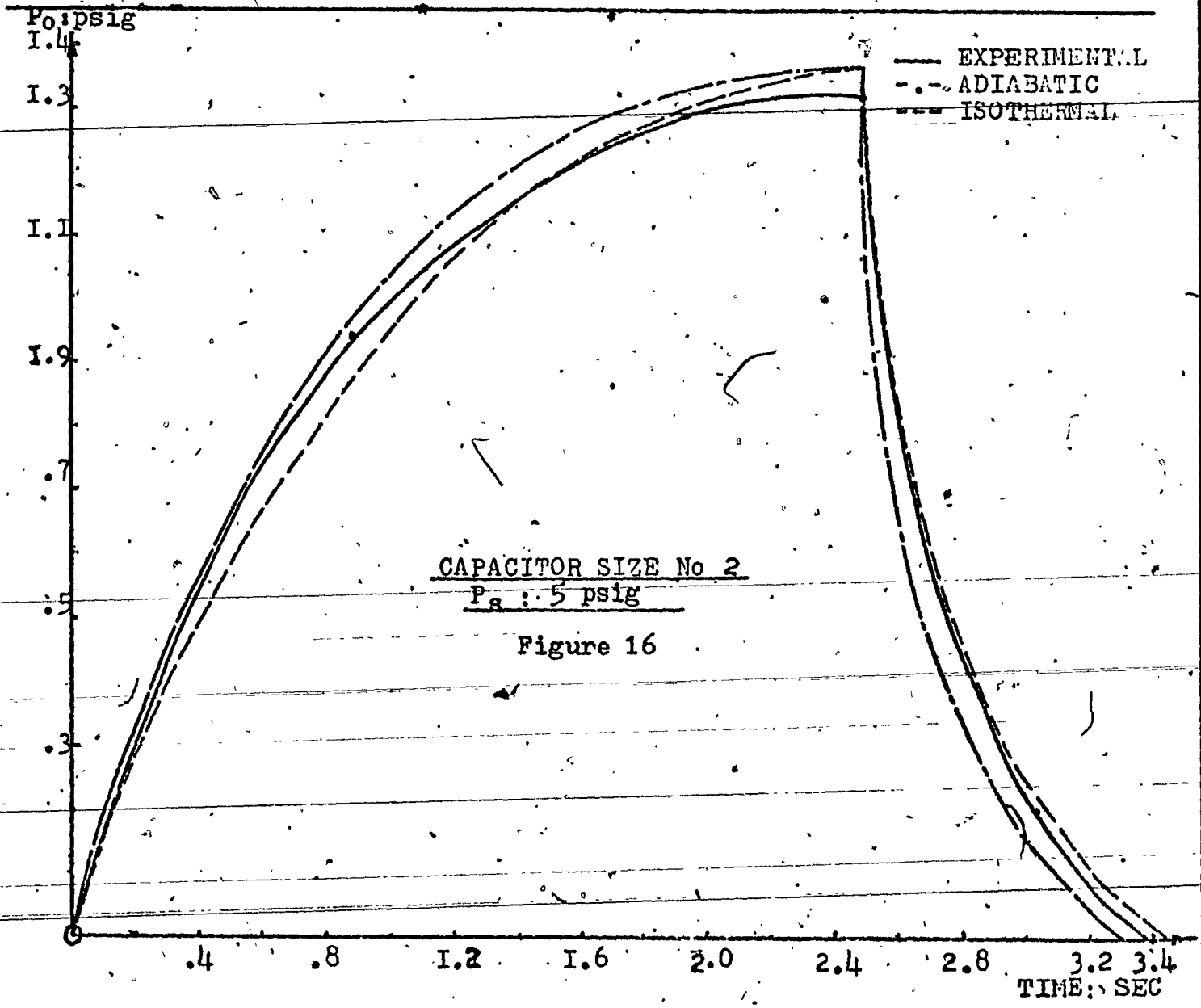

CAPACITOR SIZE No 2
P_s : 5 psig

Figure 16

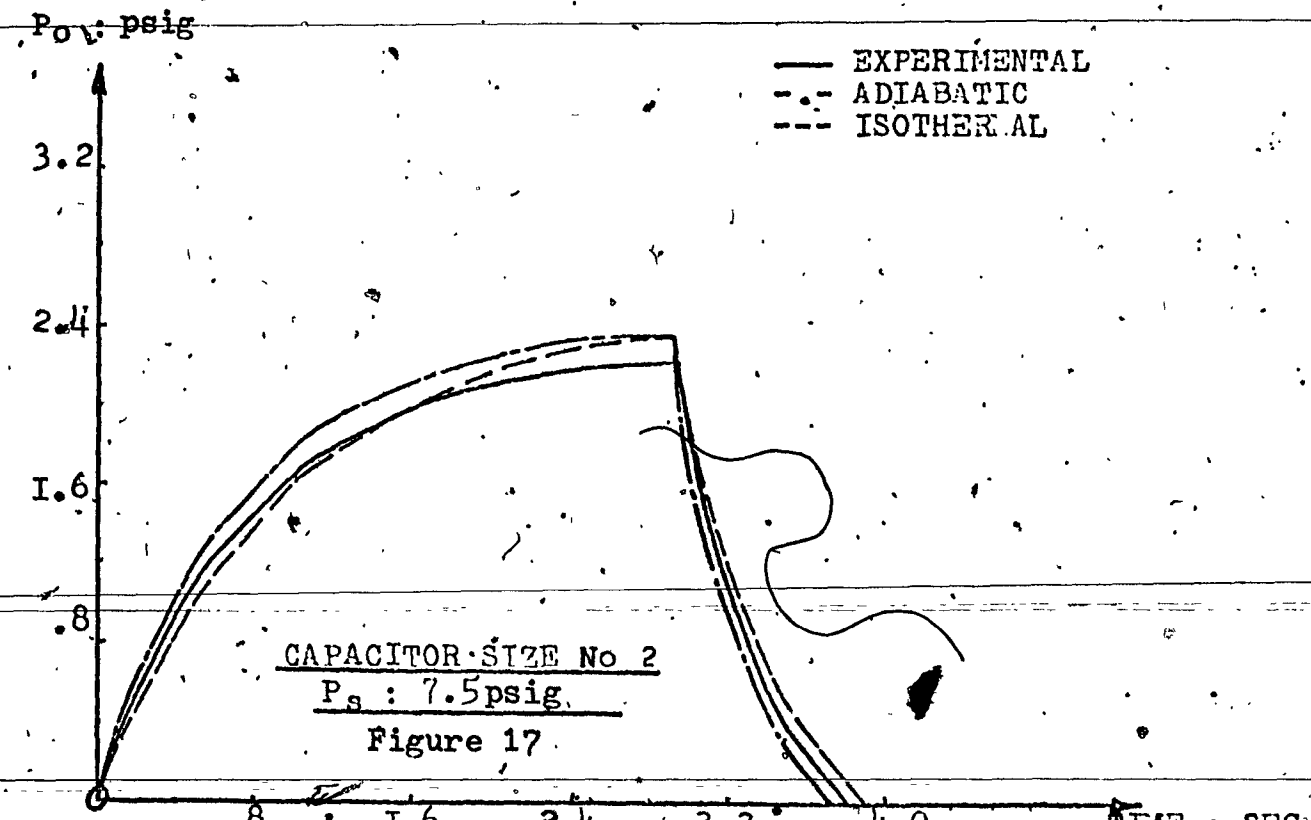

CAPACITOR SIZE No 2
P_s : 7.5psig

Figure 17

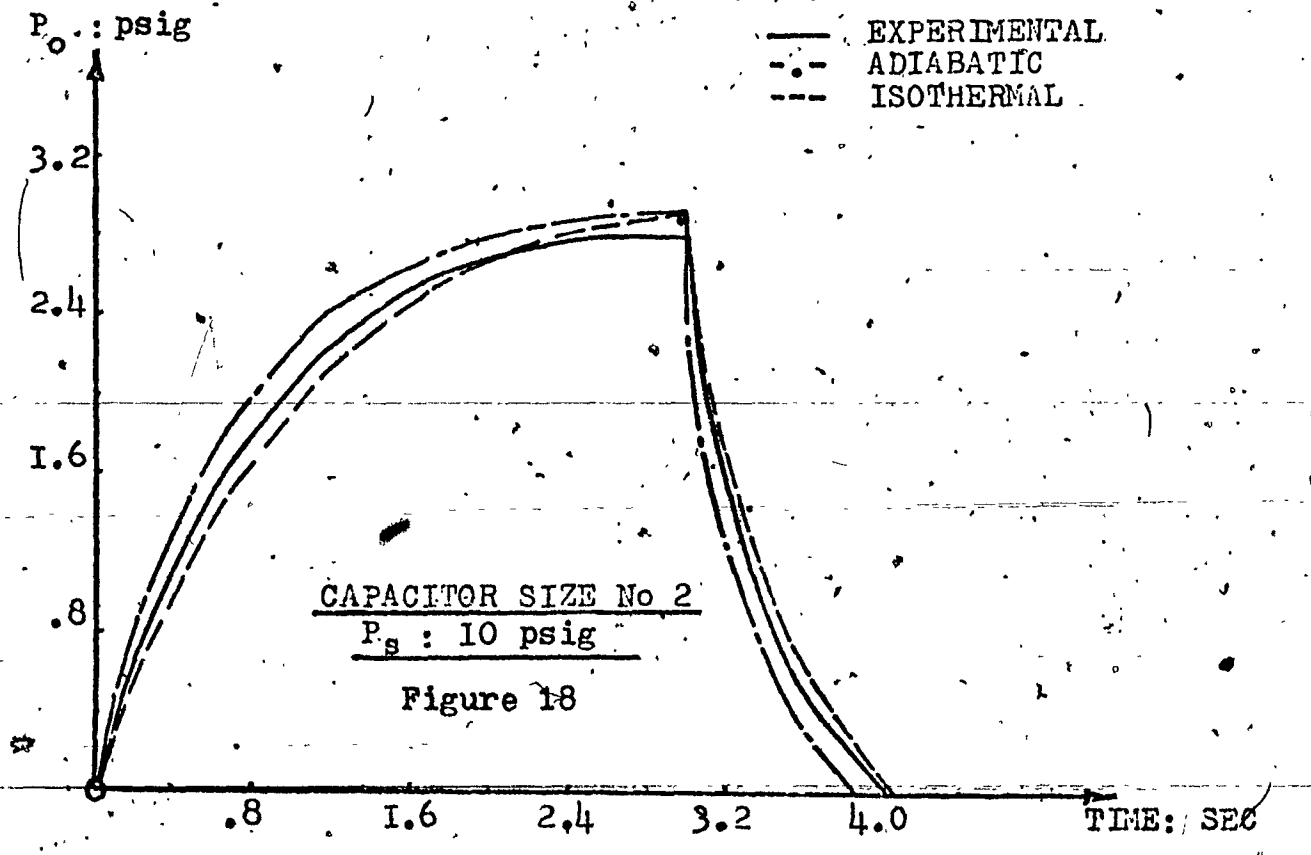

CAPACITOR SIZE No 2
P_s : 10 psig

Figure 18

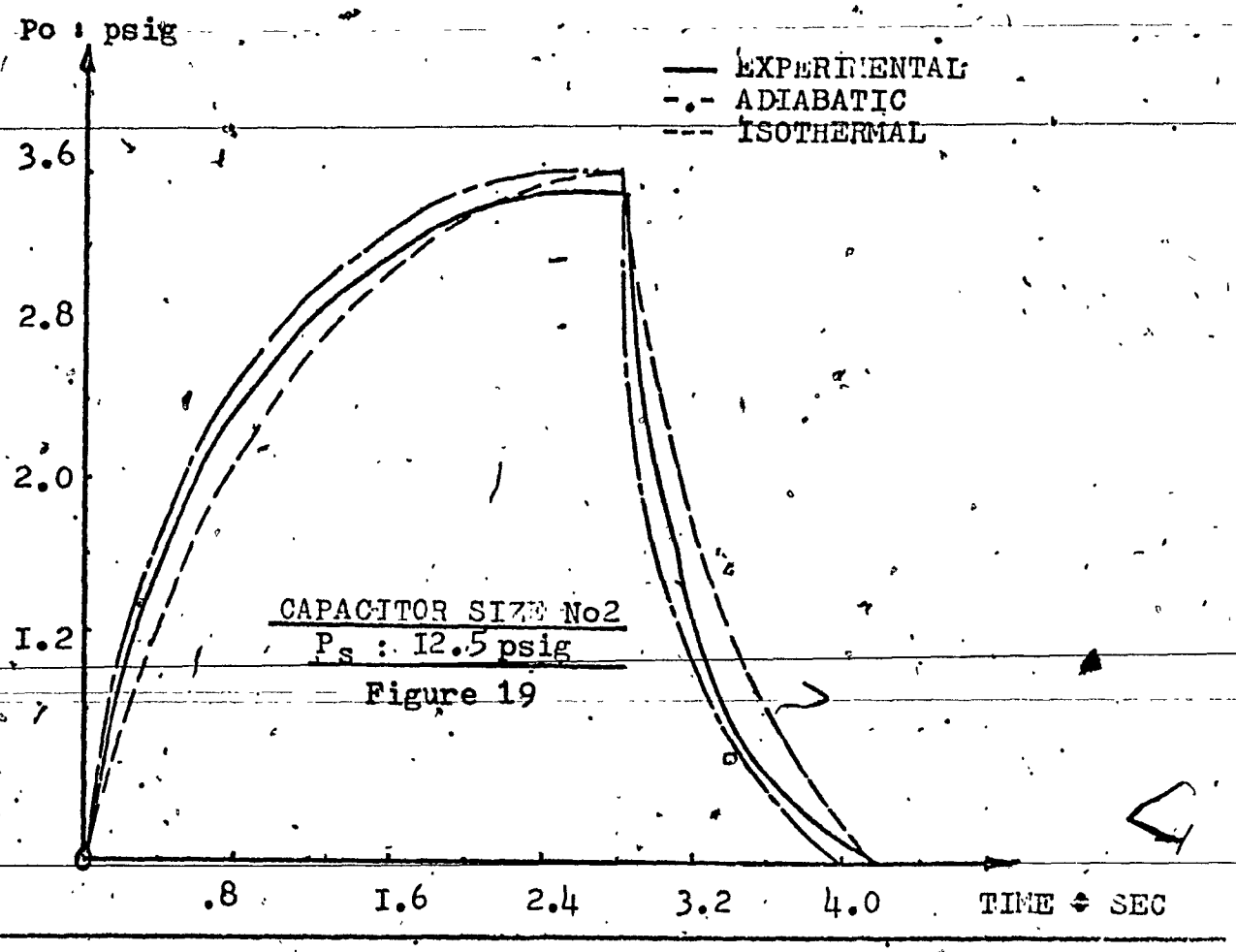

CAPACITOR SIZE No2
P_s : I2.5 psig

Figure 19

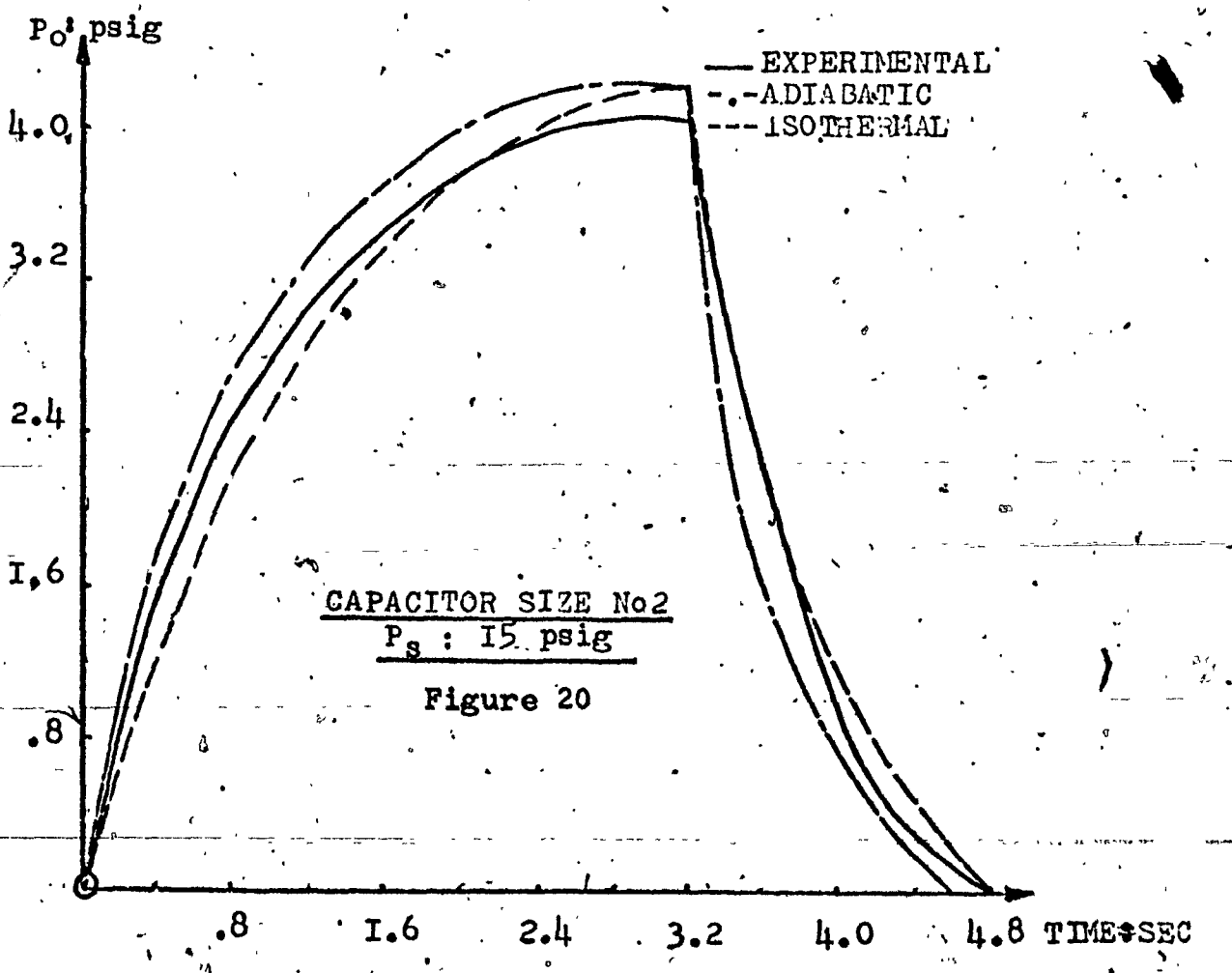

CAPACITOR SIZE No2
P_s : I5 psig

Figure 20

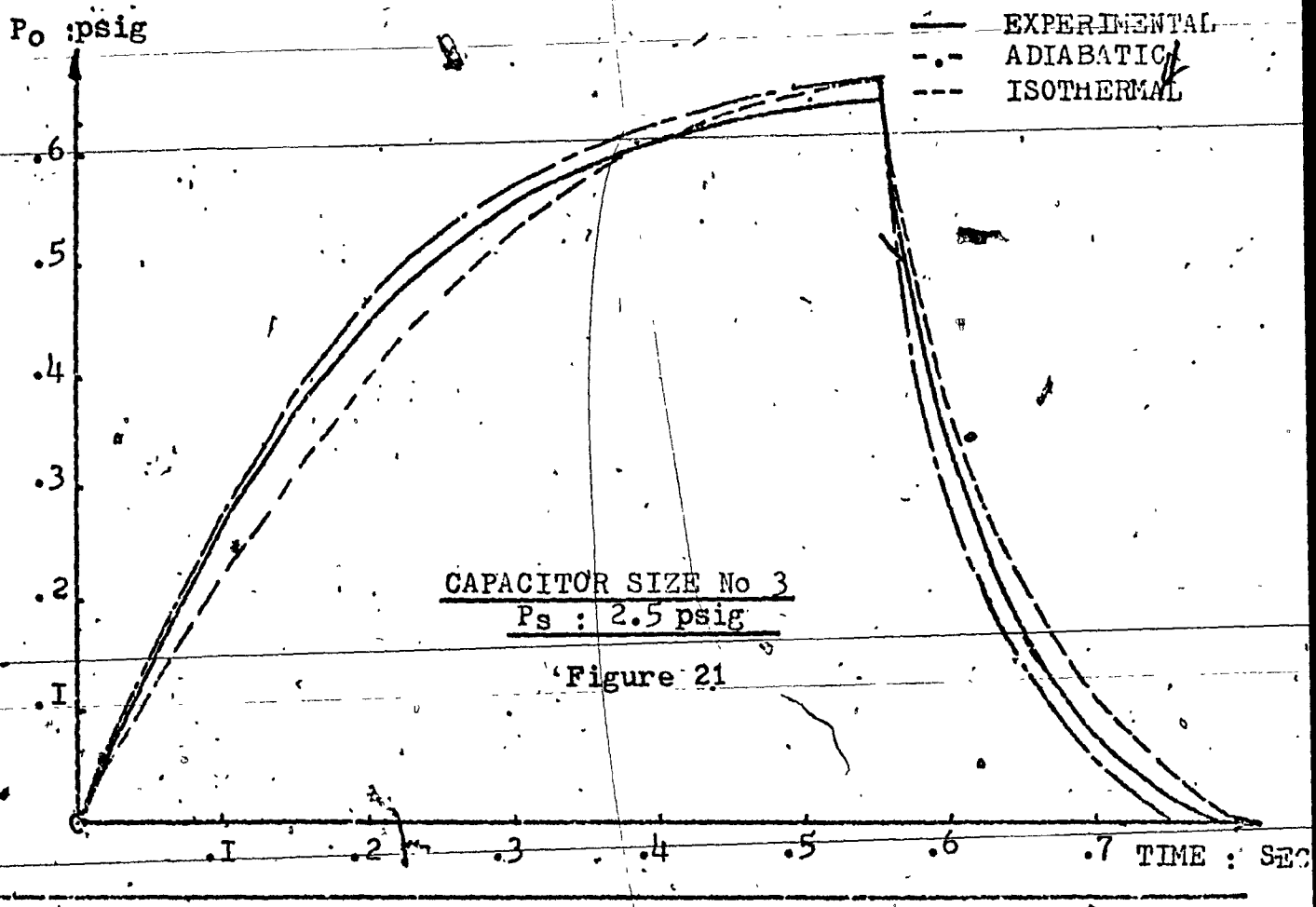

CAPACITOR SIZE No 3
P_s : 2.5 psig

Figure 21

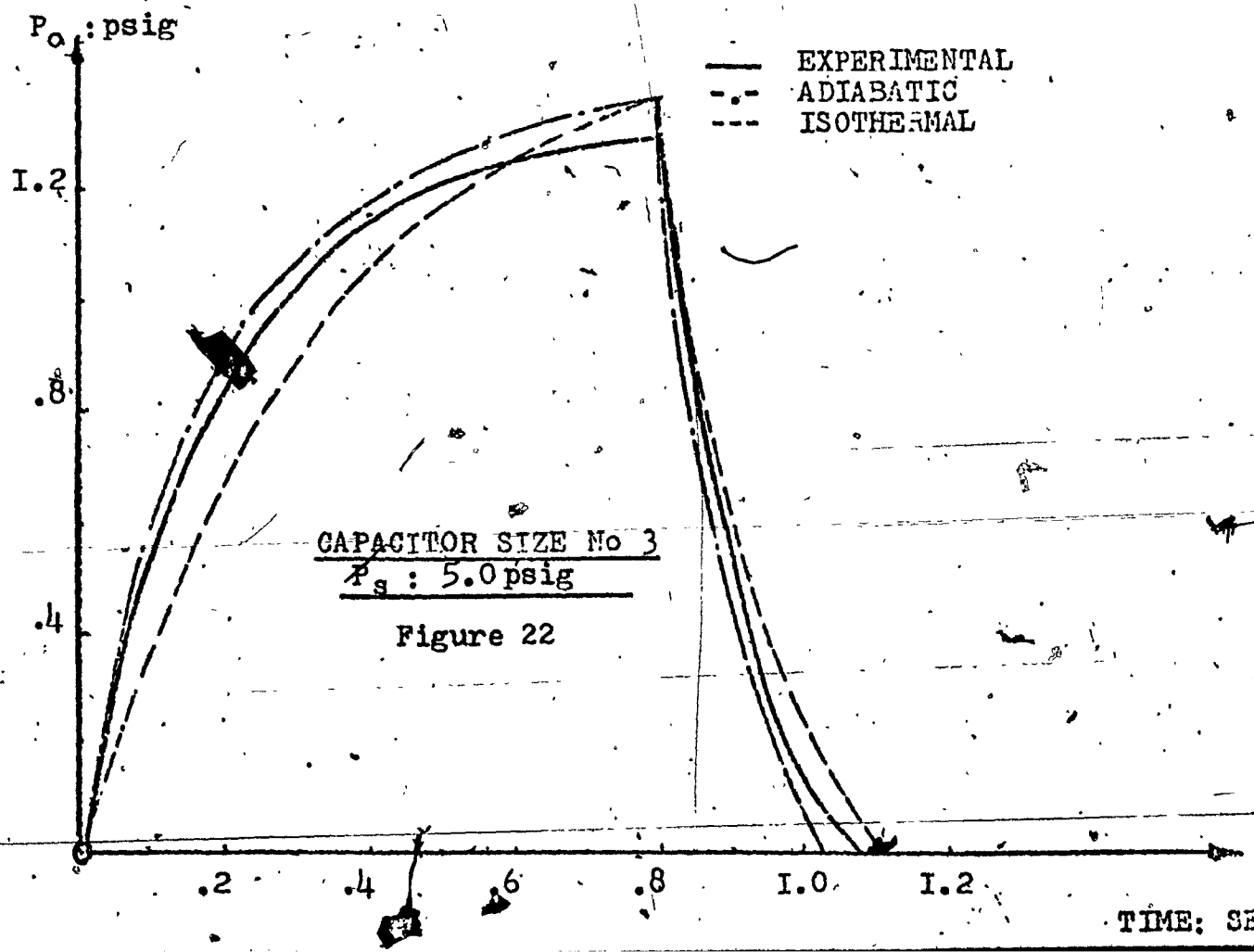

CAPACITOR SIZE No 3
P_s : 5.0 psig

Figure 22

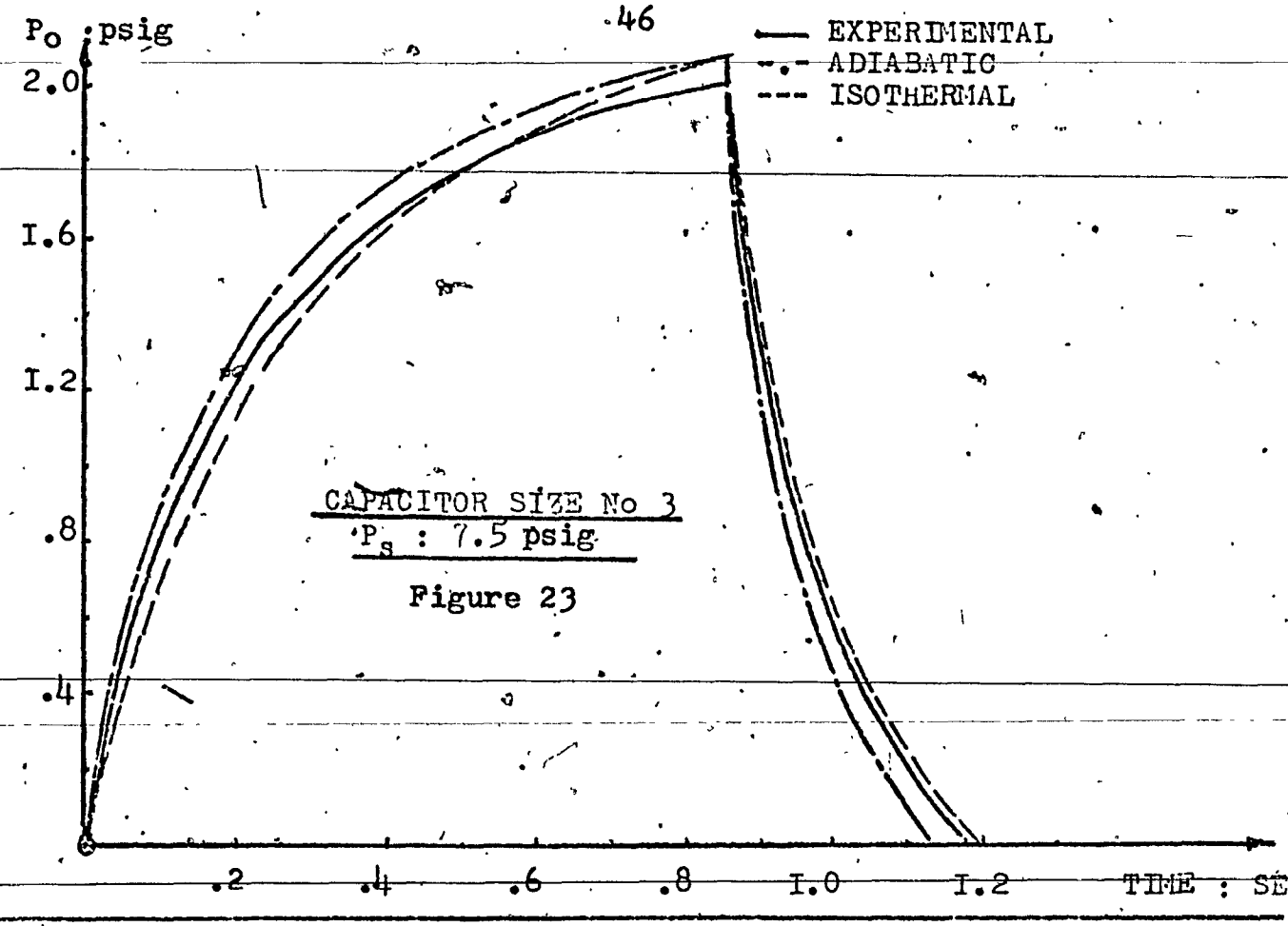

CAPACITOR SIZE No 3
P_s : 7.5 psig

Figure 23

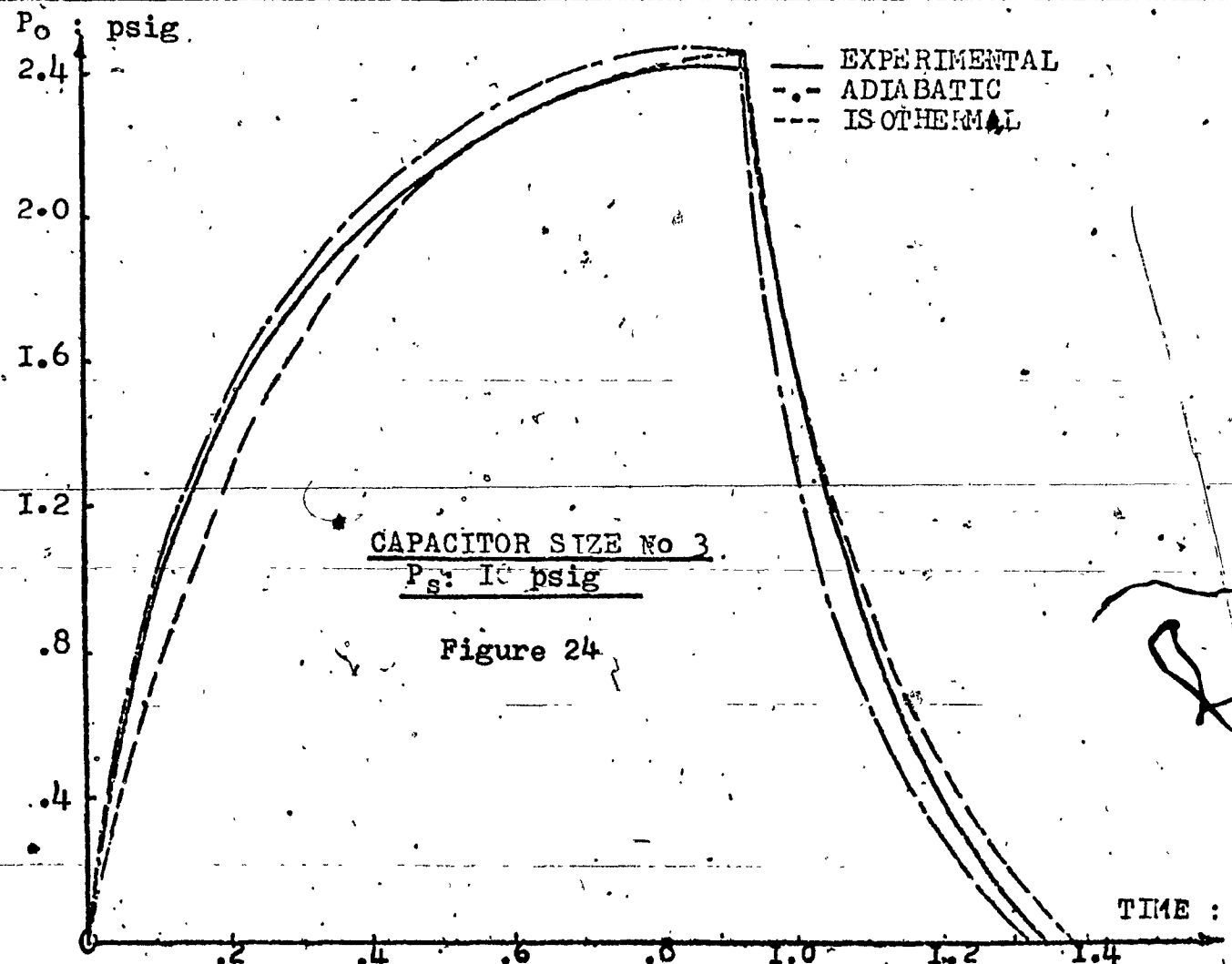

CAPACITOR SIZE No 3
P_s: 10 psig

Figure 24

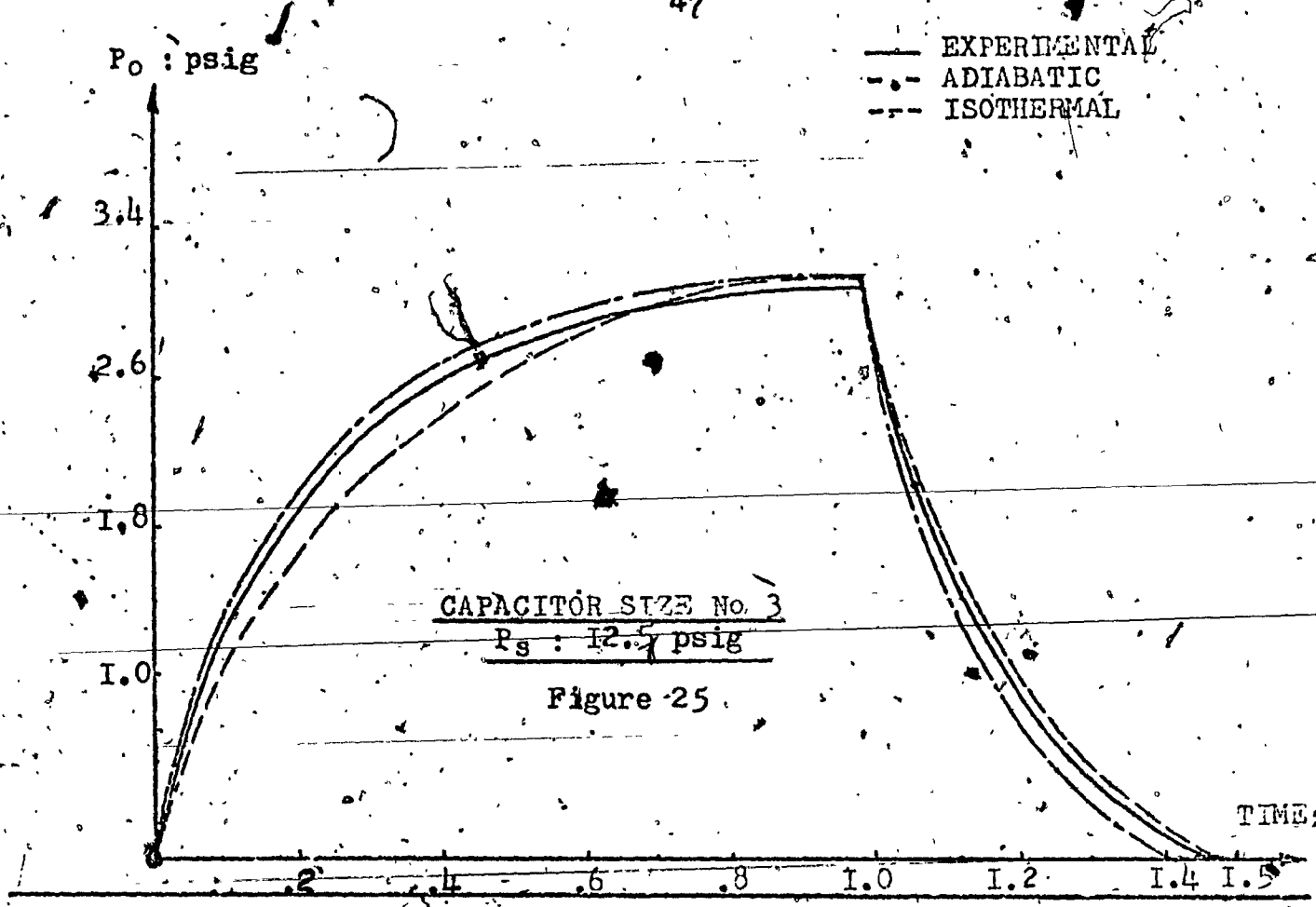

CAPACITOR SIZE No. 3
P_s : 12.5 psig

Figure 25

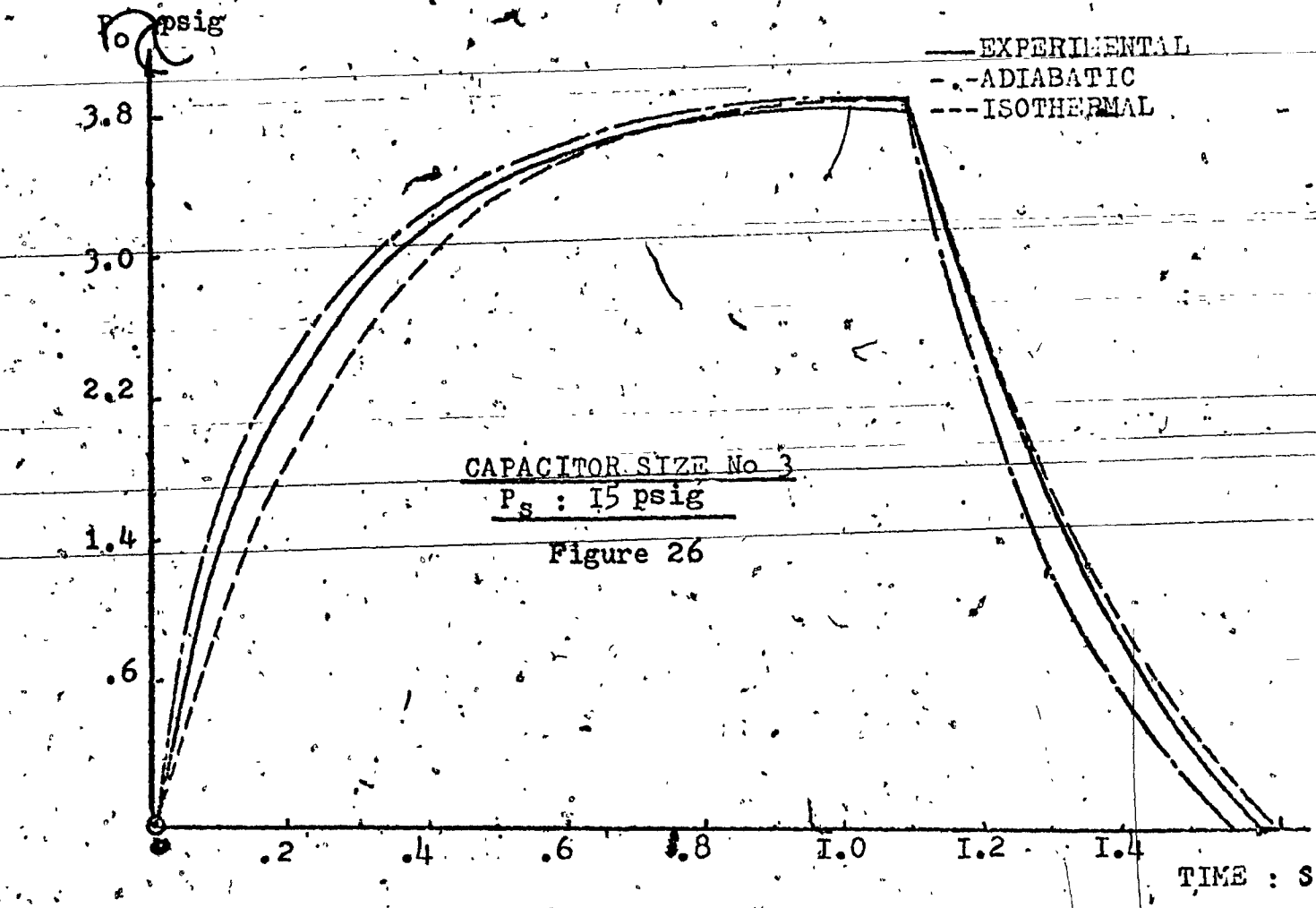

CAPACITOR SIZE No. 3
P_s : 15 psig

Figure 26

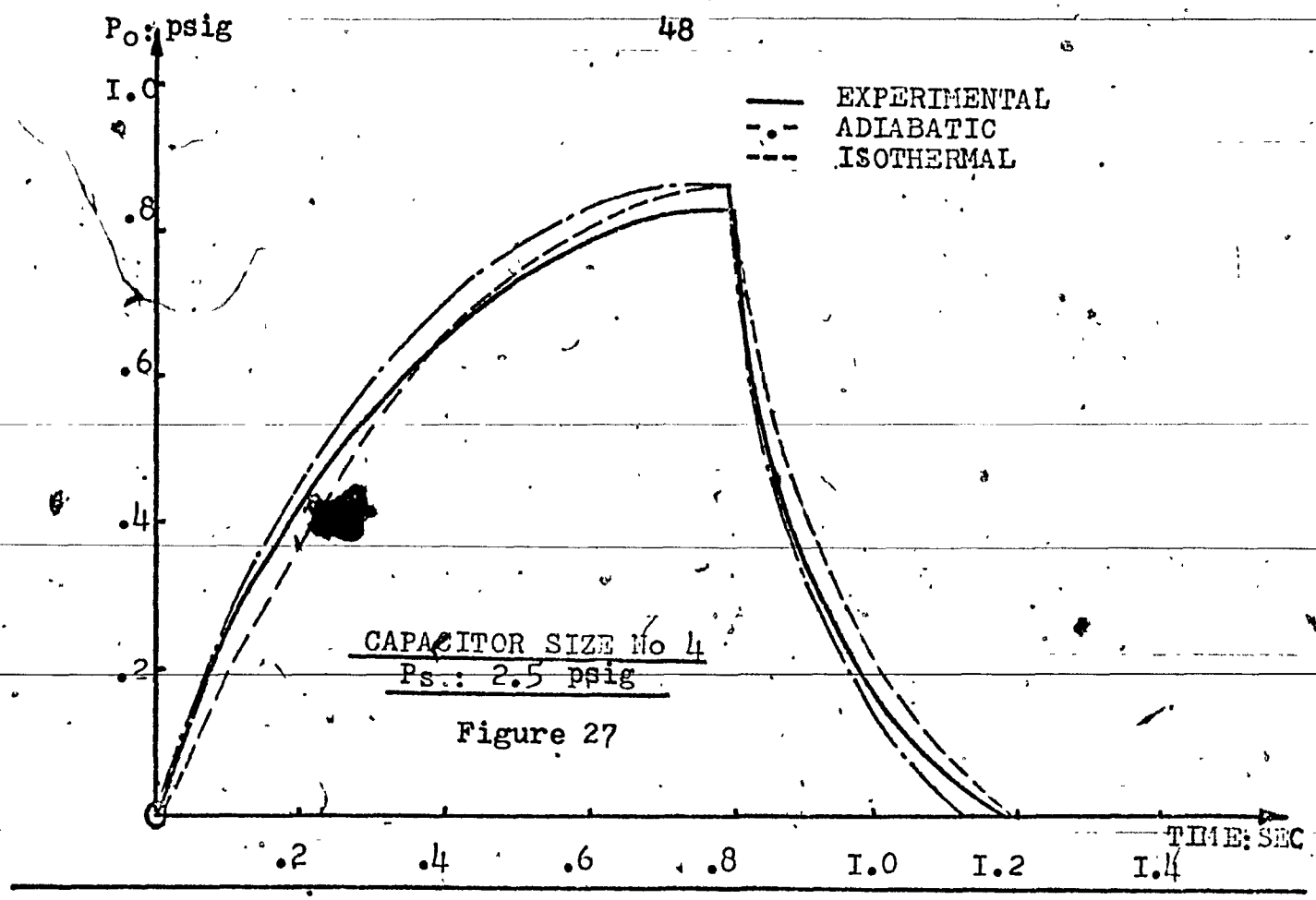

CAPACITOR SIZE No 4
P_s: 2.5 psig

Figure 27

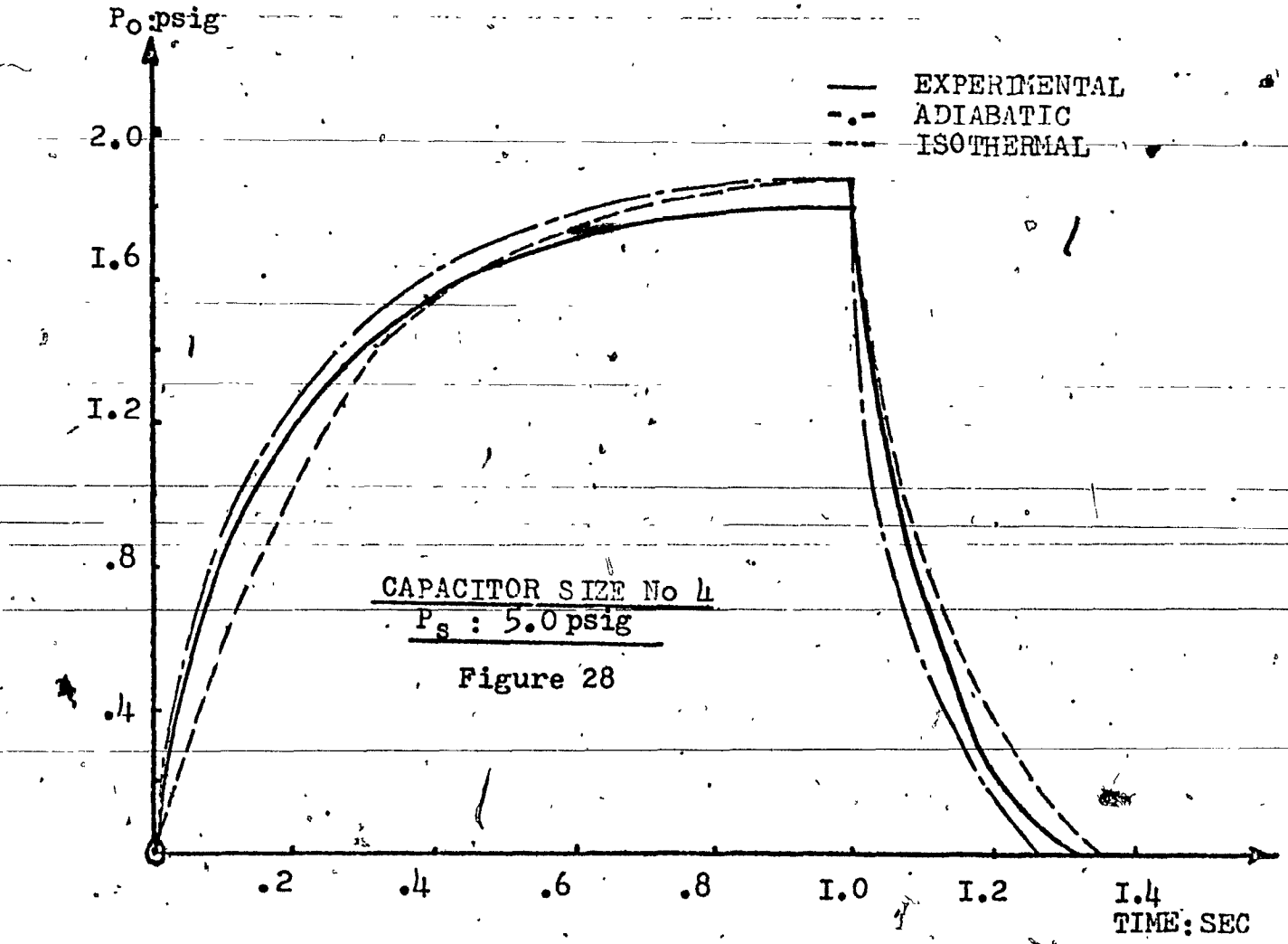

CAPACITOR SIZE No 4
P_s : 5.0 psig

Figure 28

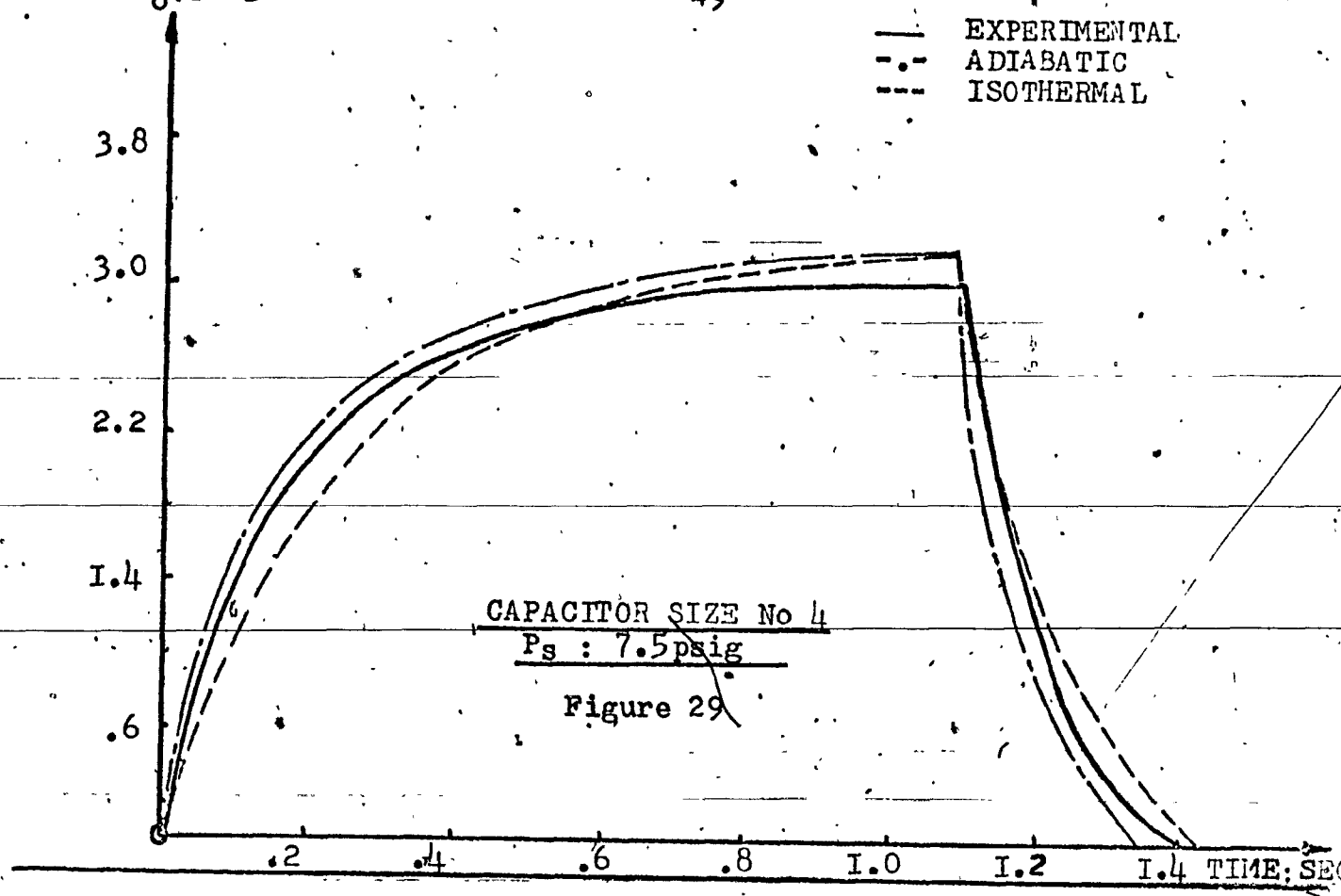

CAPACITOR SIZE No 4
Ps : 7.5psig

Figure 29

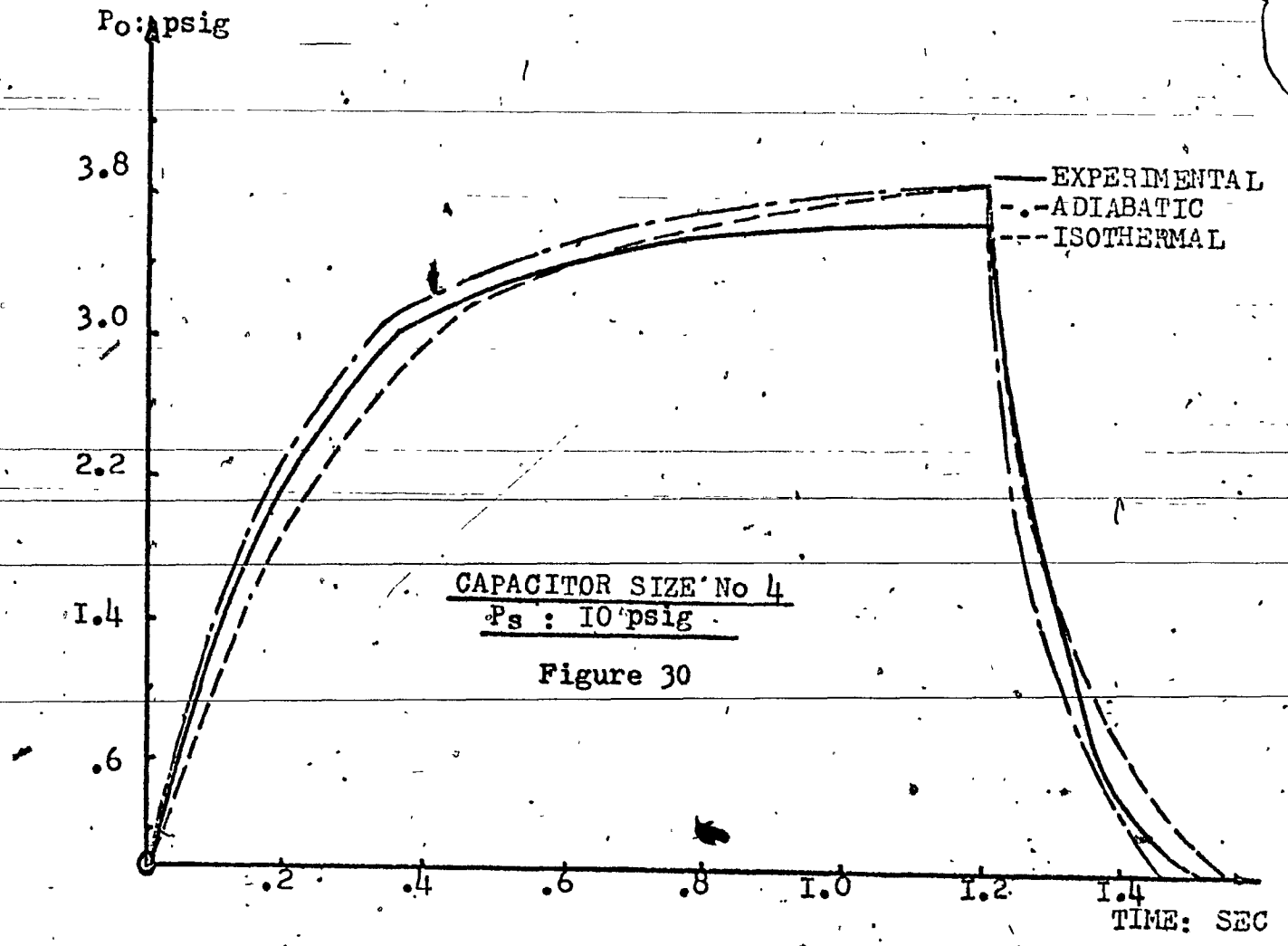

CAPACITOR SIZE No 4
Ps : IO psig

Figure 30

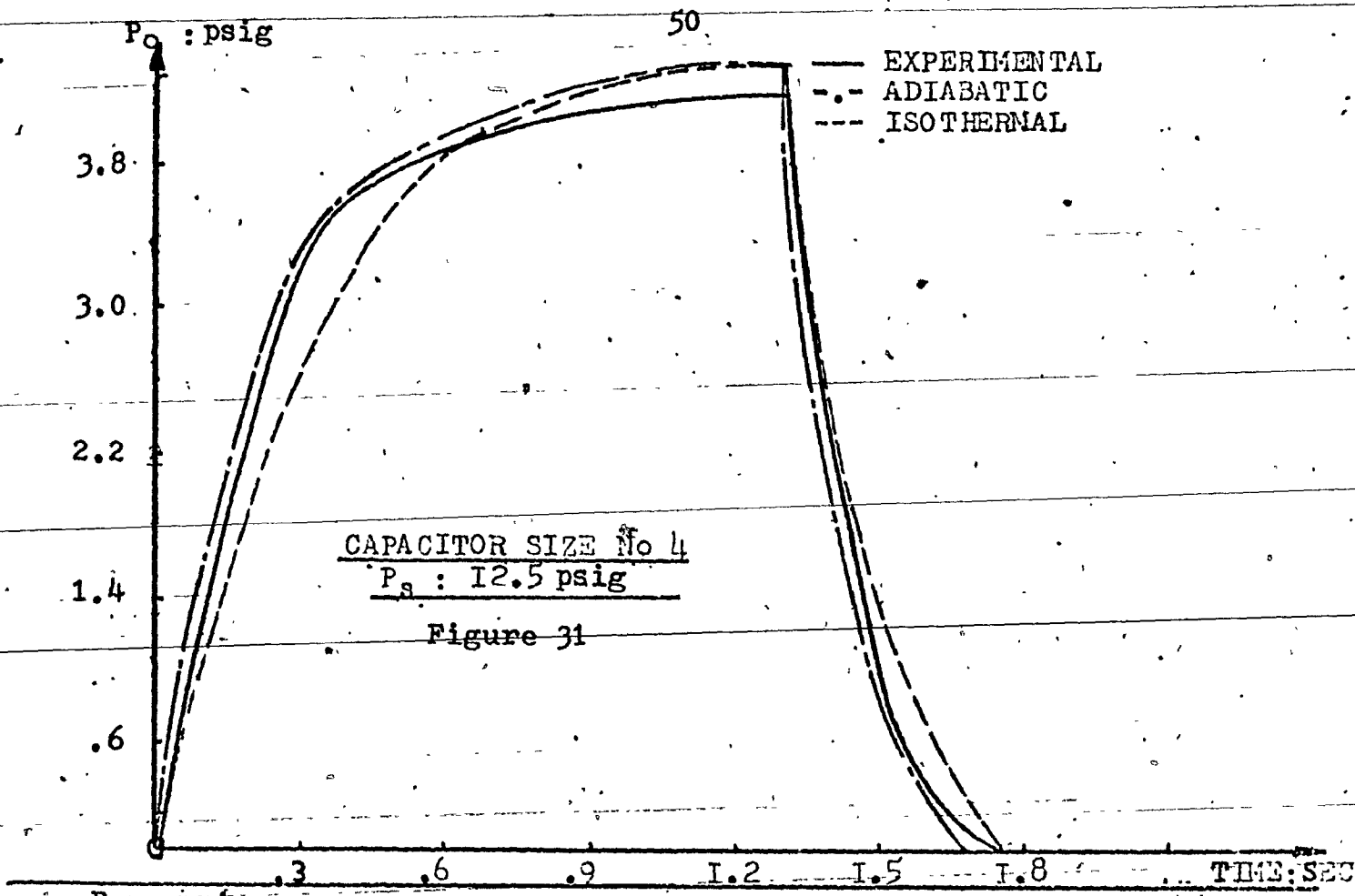

CAPACITOR SIZE No 4
P_s : 12.5 psig

Figure 31

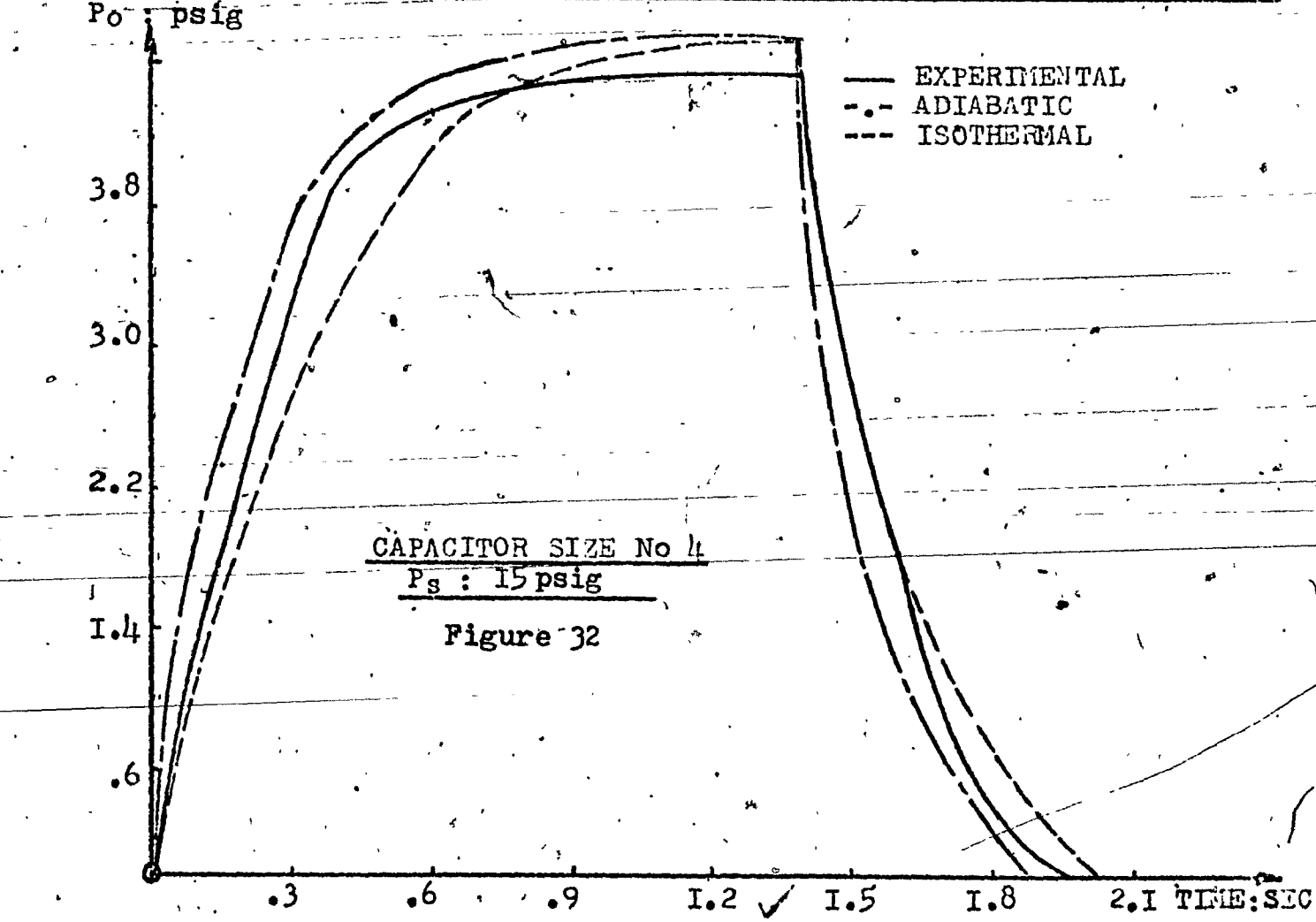

CAPACITOR SIZE No 4
P_s : 15 psig

Figure 32

APPENDIX I

FILE CATALOGUE: Fluidic Components
SECTION: Application Data I-1
TYPE: 1100MO1

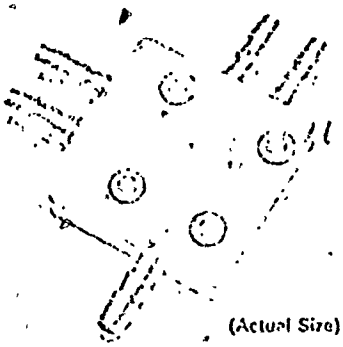
(Actual Size)

MONOSTABLE FLUID AMPLIFIER

DESCRIPTION

The Aviation Electric type 1100MO1 Monostable Fluid Amplifier is a two-input wall attachment digital control element that operates with air and most other commonly used gases. The unit provides the "or/nor" function required in digital control circuitry. The unique method of venting (patent pending) eliminates the impedance matching and satisfaction switching problems usually associated with no-moving parts fluid amplifiers and permits the straightforward design of pneumatic circuitry using standard off-the-shelf components.

OPERATING CHARACTERISTICS

Function: Two-input Monostable Flip-Flop

Operating Medium: Gaseous Fluids

Operating Principle: Wall Attachment

Temperature Range: −140°F to +270°F.

	MAXIMUM	NOMINAL	MINIMUM
Input Pressure.	15 psig	2.5 psig	1.0 psig (See Fig. 1)
Power Consumption		1.1 watts	
Pressure Recovery (blocked)		42%	
Flow Recovery (unblocked)		125%	
Frequency Response		800 cps	
Response Time		0.0004 sec.	
Switching Pressure		0.35 psi max.	

Loading Capacity: Element is stable with zero inactive leg flow from fully opened to fully blocked conditions on the active leg. (See Fig. 2)

Note: Detailed operating characteristics given on the reverse side of this data sheet.

APPLICATIONS

This device has been designed for use in digital and pulse processing fluidic circuits which may be built up in the same way as electronic circuits using solid-state, "or/nor" flip-flops. The use of fluidics represents a cost saving and reliability improvement over conventional electronics, and is particularly advantageous in applications where temperature, radiation, shock, vibration, or explosion hazards rule out the choice of electronic/electric circuitry.

SPECIFICATIONS

Dimensions: See drawing on reverse side of sheet

Material: Polycarbonate Thermoplastic

Fittings: Tri-serrated brass suitable for ⅛" I.D. flexible tubing.

Compatibility: Compatible with most common gases, water, oils, acids and alcohols.

Engineering services are available to review applications feasibility.

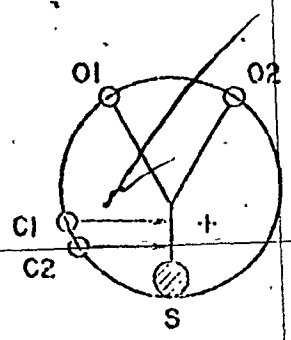

S= SUPPLY

C1 , C2 = INPUTS

O1 = $\overline{C1} \cdot \overline{C2}$ = OUTPUT

O2 = C1 + C2 = OUTPUT

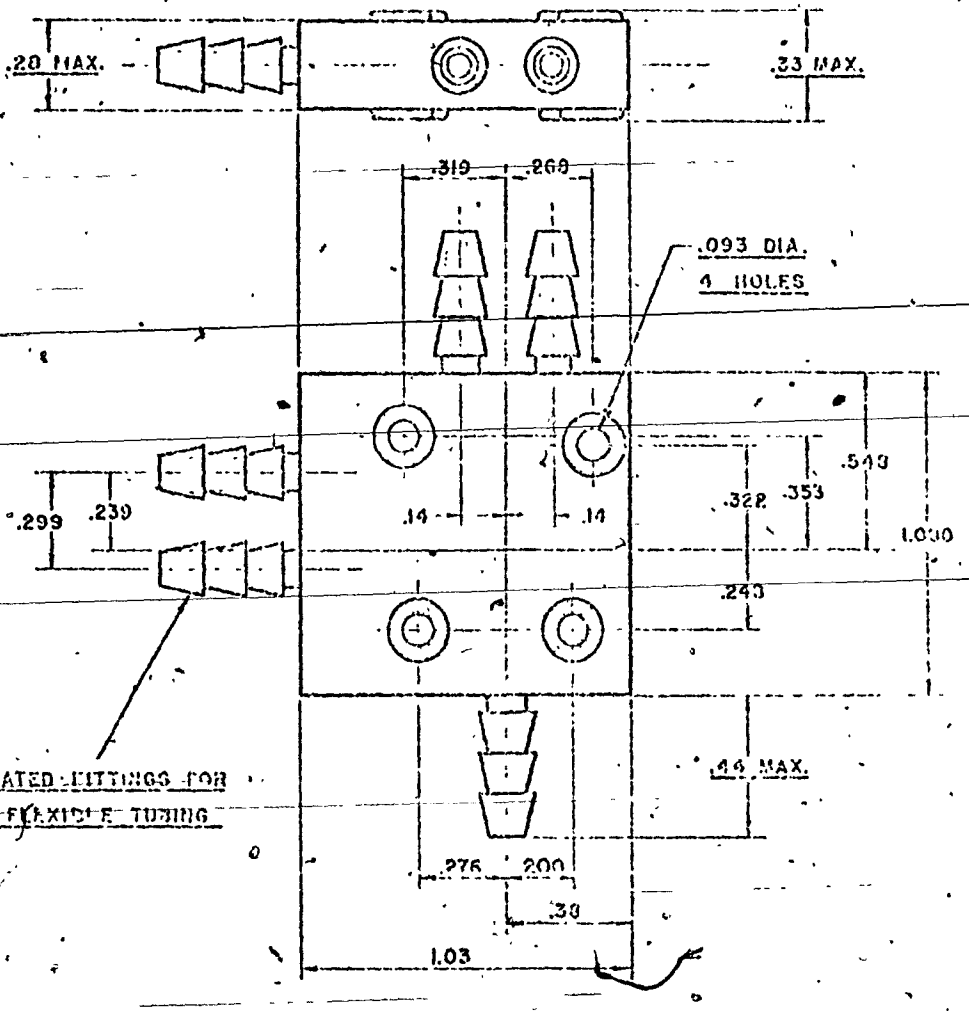

OUTPUT AND LOADLINE CHARACTERISTICS

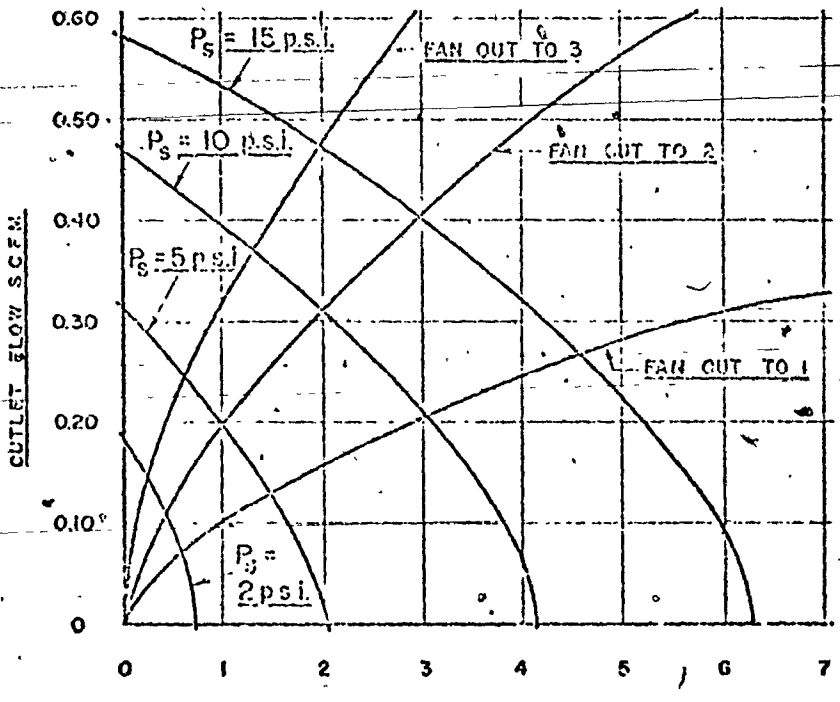

FIGURE 2

SUPPLY PRESSURE AND FLOW CHARACTERISTICS

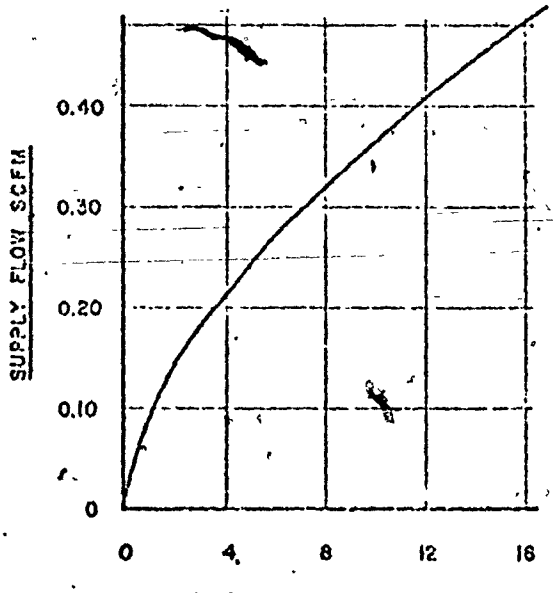

FIGURE 1

APPENDIX II

PROCEDURE FOR DETERMINING THE FLUID AMPLIFIER CHARACTERISTICS

2.1 The Output Characteristics

The pressure-flow characteristic curves for the charging amplifier No. 1 (AE 1100M01) were obtained for its output leg "01" which is a normally active output port for the monostable amplifier. This output is used later to connect the amplifier with the input of the capacitor. The pressure-flow characteristics were obtained by gradually loading the output port 01 and then measuring the instantaneous pressure upstream of the load and the flow recoveries at the exit (see Figs. 2a and 3).

2.2 The "Reverse Flow" Characteristic

In order to obtain the reverse flow characteristics through leg "01" (see Figs.2b and 4a), one of the control jets must be active so that the output of the amplifier will be diverted to leg "02". This was achieved by switching ON the ON-OFF switch to the control port "C1". The pressure-flow characteristics were obtained by gradually increasing the pressure at 01 and then measuring the instantaneous pressure and flow through the leg "01".

Back-pressure corrections were incorporated into the flow-meter readings, thus reducing the flow rate to standard cubic feet per minute, scfm.

2.3 The "Load Line" Pressure Flow Characteristics

The amplifier is connected through its supply port to a constant supply pressure (see Figs.2c and 4b). Its control port C1 was connected to another pressure supply via a flowmeter. The load line pressure-flow characteristics were then obtained by gradually increasing the pressure at C1 and then measuring the instantaneous pressure and flow through the control port C1. Errors due to back-pressure effects on the flowmeter readings were appropriately corrected.

APPENDIX III

EXPERIMENTAL DETERMINATION OF THE SPRINGS CONSTANT OF THE BELLOWS.

In order to determine the spring constant of the bellows the following relationship was used.

$$Ps\ Aeq = K\ X$$

where,

Aeq : The equivalent cross-section area of the bellows - IN^2

Ps : The supply pressure to the bellows - psig

K : The spring constant of the bellows - LBf/IN

X : Linear desplacement of the bellows - IN.

The numerical evaluation of K from the above mentioned relationship was determined as follows:

A known pressure was applied to the bellows and the corresponding linear displacement was measured. After applying successive known pressures and measuring the corresponding linear-displacements, graphs were plotted (Fig. 7 and 8) showing the relation between pressure and displacement. The slope of the curves represents the bellows spring constant K.

It can be seen from the curves that the value of the spring constant K of each particular bellows remains constant. Furthermore, it should be noted that during the experiment the supply air and the room air temperatures were constant.